

Platonic dynamical decoupling sequences for qudits

Colin Read, Eduardo Serrano-Ensástiga, and John Martin

Institut de Physique Nucléaire, Atomique et de Spectroscopie, CESAM, University of Liège
B-4000 Liège, Belgium

In the NISQ era, where quantum information processing is hindered by the decoherence and dissipation of elementary quantum systems, developing new protocols to extend the lifetime of quantum states is of considerable practical and theoretical importance. A prominent method, called dynamical decoupling, uses a carefully designed sequence of pulses applied to a quantum system, such as a qudit (a d -level quantum system), to suppress the coupling Hamiltonian between the system and its environment, thereby mitigating dissipation. While dynamical decoupling of qubit systems has been widely studied, the decoupling of qudit systems has been far less explored and often involves complex sequences and operations. In this work, we design efficient decoupling sequences composed solely of $SU(2)$ rotations and based on tetrahedral, octahedral, and icosahedral point groups, which we call Platonic sequences. We use a generalization of the Majorana representation for Hamiltonians to develop a simple framework that establishes the decoupling properties of each Platonic sequence and show its efficiency on many examples. These sequences are universal in their ability to cancel any type of interaction with the environment for single qudits with up to 6 levels, and they are capable of decoupling up to 5-body interactions in an ensemble of interacting qubits with only global pulses, provided that the interaction Hamiltonian has no isotropic component, with the exception of the global identity. We also discuss their inherent robustness to finite pulse duration and a wide range of pulse errors, as well as their potential application as building blocks for dynamically corrected gates.

1 Introduction

Many quantum hardware devices are limited by the coherence time of their noisy constituents due to undesirable interactions among them or with their environment. These interactions lead to decoherence and

Colin Read: cread@uliege.be

Eduardo Serrano-Ensástiga: ed.ensastiga@uliege.be

John Martin: jmartin@uliege.be

dissipation and, consequently, to a deterioration of the overall quantum state, which contains the useful information to be processed, stored, and extracted. In a world where quantum error correction is not yet available to correct this loss of information, the development of protocols to mitigate undesirable interactions is of major practical interest [1, 2], but also of fundamental theoretical importance. In particular, such protocols can be useful in emergent quantum technologies or for revealing minute physical effects masked by surrounding noise [1].

A well-known technique for mitigating decoherence is called dynamical decoupling (DD) and consists of applying a periodic sequence of pulses to the system of interest in order to average out its unwanted interaction with the environment. Since Viola's seminal work [3], numerous DD sequences have been constructed and optimised, firstly for a single qubit [4–7] and then for multiqubit systems [8–11]. They have been successfully implemented on a variety of physical platforms, such as NV centers in diamond [12], trapped ions [6] or superconducting flux qubits [13]. They are routinely used in experiments such as NMR and electron spin resonance to reduce decoherence, but also to measure transverse relaxation times more accurately [14] or to finely probe the local spin environment in systems of interacting spins [15].

Dynamical decoupling of qudit ensemble has been much less explored. A universal DD sequence for a single qudit based on the Heisenberg-Weyl group was recently constructed and experimentally implemented [16]. Some sequences were constructed from orthogonal arrays which were shown to decouple an ensemble of interacting qudits, assuming that individual control over each qudit is possible [17–20]. However, the complexity of these protocols increases drastically with the number of qudits in the ensemble; more recent work has relied on numerical approaches to solve this issue [21, 22].

In this work, we demonstrate the decoupling properties of three sequences based on exceptional point groups, namely the Tetrahedral, Octahedral and Icosahedral point groups. They correspond to the Eulerian sequences derived from the Cayley graphs of these groups [4, 23]. These novel sequences, which we call *Platonic DD sequences*, decouple several types of interactions in multiqudit systems, depending on the $SU(2)$ irreducible representations (irreps) of the unwanted system-environment Hamilto-

nian. We use Majorana representation of (Hermitian) operators [24,25] to systematically calculate the possible point groups of a general interaction Hamiltonian for qudits with different numbers of levels. Once we generalize this representation to arbitrary operators, we can deduce the interactions that each Platonic sequence can decouple.

Throughout this work, we use the equivalence between an arbitrary d -level quantum system (qudit) and a spin- j with spin quantum number $j = (d-1)/2$, for which the structure of irreps of $SU(2)$ emerges naturally. But we emphasise that our results apply to any multipartite quantum system as long as there are feasible unitary operations corresponding to $SU(2)$ transformations acting globally, *i.e.*, the *same* operation is applied to each constituent of the system. The most common experimental implementation of the $SU(2)$ group is through physical rotations that can be induced, for example, by applying a magnetic field to a spin, whether electronic or nuclear, as in NMR [26]. However, there are different $SU(2)$ implementations in other physical platforms such as multiphoton systems [27,28] or two-component Bose-Einstein condensates [29].

This paper is organized as follows. In Sec. 2, we describe the necessary mathematical tools, introducing the different point groups and the decomposition of Hilbert spaces into $SU(2)$ irreps¹. In Sec. 3, we introduce the Majorana representation of Hermitian and non-Hermitian operators and systematically study their possible point groups. In particular, we define and list the set of largest point groups for different types of Hamiltonians corresponding to different irreps. In Sec. 4, we recall the necessary notions of dynamical decoupling. Then, using the results of Sec. 3, we develop a framework for selecting the relevant decoupling groups for a single spin- j system (Sec. 5) and a multispin system (Sec. 6), focusing on the Platonic DD sequences. We study the robustness of these sequences with respect to various pulse errors in Sec. 7. Finally, we discuss their potential application for dynamically corrected gates in Sec. 8 and conclude with a summary and outlook in Sec. 9.

2 Mathematical tools

In this section, we present some general reminders about point groups and representation theory of Hilbert spaces which are useful for this work.

¹We use the usual convention of calling $SU(2)$ j -irrep both the respective set of $(2j+1) \times (2j+1)$ matrices defining the action of the group elements, and the $(2j+1)$ -dimensional vector space where the action of the group is defined through the same matrices.

2.1 Point groups

Point groups in three dimensions are classified into different families denoted in the Schönflies notation [30, 31] as: the axial groups $C_n, S_{2n}, C_{nh}, C_{nv}, D_n, D_{nd}, D_{nh}$ and the polyhedral groups $T, T_d, T_h, O, O_h, I, I_h$. In this work, we only consider proper point groups, *i.e.*, those not containing reflections. Any of these point groups can be generated by only two rotations, also called abstractly generators (see Appendix A for more details). We denote by C_n^k a $2\pi k/n$ rotation about an axis. We now describe briefly every proper point group:

i) *Cyclic groups* C_n : such groups have n elements consisting of $2\pi q/n$ rotations along the same axis of rotation, where $q = 0, 1, \dots, n-1$. Regular polygons on the sphere that do not lie in a great circle² have this symmetry. In addition, there is one group of infinite order, denoted C_∞ , consisting of the subgroup of rotations about a fixed axis by any angle (the symmetry of a point on the sphere). Each C_n has only one generator C_n .

ii) *Dihedral groups* D_n : For $n \geq 2$, they contain $2n$ elements: n rotations C_n over the principal axis, and n additional C_2 rotations about axes perpendicular to the principal axis. This is the proper point group of a regular prism with $n > 2$ sides, antiprisms³ (with $n > 3$) and regular n -gons on a great circle of the sphere for $n > 2$. The group D_∞ has as subgroup C_∞ on a principal axis of rotation, as well as any rotation of π about an axis perpendicular to it. It is equivalent to the point group associated with a pair of antipodal points. Each D_n has two generators: C_2 and C_n .

iii) *Tetrahedral group* T : It consists of 12 elements $T = \{E, 8C_3, 3C_2\}$ corresponding to the rotations which leave a regular tetrahedron invariant. A possible set of generators of T consists of two C_3 rotations about different axes.

iv) *Octahedral group* O : It consists of 24 elements $O = \{E, 8C_3, 9C_2, 6C_4\}$ which transform a regular octahedron (or cube) into itself. It can be generated by a C_3 and a C_4 rotation.

v) *Icosahedral group* I : It consists of 60 elements $\{E, 12C_5, 12C_5^2, 20C_3, 15C_2\}$ and is equivalent to the symmetry point group of a regular icosahedron (or dodecahedron). It has two generators: C_3 and C_5 .

The point group notation is abstract in the sense that it does not specify the orientation of the axes. A procedure for constructing the three exceptional groups (T , O and I) from their generators is presented in Appendix A. The corresponding Cayley graphs are presented in Appendix B.

²The circles on the sphere whose center coincides with the center of the sphere are called *great circles*.

³An antiprism with n sides has a point group D_n unless it is a tetrahedron or octahedron (Platonic solids for $n = 2, 3$), respectively.

2.2 Representation theory of Hilbert spaces

Let us consider a general quantum state $|\Psi\rangle \in \mathcal{H}$ in a finite-dimensional Hilbert space \mathcal{H} where the elements of the rotation group $\mathbf{R} \in \text{SO}(3)$ are represented by the unitary operators $\mathbf{R}(\mathbf{n}, \theta) = e^{-i\theta \mathbf{n} \cdot \mathbf{J}}$, with $\mathbf{n} = (n_x, n_y, n_z)$ and θ the axis-angle parameters, and $\mathbf{J} = (J_x, J_y, J_z)$ the angular momentum operator of the quantum system. From representation theory, the Hilbert space \mathcal{H} has a decomposition into subspaces which transform independently under a $\text{SU}(2)$ transformation as one of its irreps, *i.e.*,

$$\mathcal{H} = \bigoplus_{(j, \alpha_j)} \mathcal{H}^{(j, \alpha_j)} \quad (1)$$

where the superindex (j, α_j) is used to label spin- j irreps of dimension $2j+1$, with α_j an additional integer index used to distinguish between different subspaces of the same dimension. For example, for a two-qubit system, we have $\mathcal{H} = \mathcal{H}^{(0)} \oplus \mathcal{H}^{(1)}$ because there is no degenerate irrep, whereas for a three-qubit system, we have $\mathcal{H} = \mathcal{H}^{(1/2, 1)} \oplus \mathcal{H}^{(1/2, 2)} \oplus \mathcal{H}^{(3/2)}$. In the following, we explain our method for a single spin- j system with $\mathcal{H} = \mathcal{H}^{(j)}$.

Similarly, the space of Hilbert–Schmidt operators⁴ $\mathcal{B}(\mathcal{H}^{(j)})$ can be decomposed into subspaces that transform as $\text{SU}(2)$ irreps,

$$\mathcal{B}(\mathcal{H}^{(j)}) = \bigoplus_{L=0}^{2j} \mathcal{B}^{(L)}, \quad (2)$$

where each spin- L irrep $\mathcal{B}^{(L)}$, or simply L -irrep, appears only once. Each L -irrep is spanned by multipolar operators, $\mathcal{B}^{(L)} = \text{span}(\{T_{LM}\}_{M=-L}^L)$ [32, 33]. The complete set $\{T_{LM} : L = 0, \dots, 2j; M = -L, \dots, L\}$ forms an orthonormal basis of $\mathcal{B}(\mathcal{H}^{(j)})$ with respect to the Hilbert–Schmidt inner product. By definition, multipolar operators transform according to the spin- L irrep under rotations $\mathbf{R} \in \text{SO}(3)$, *i.e.*,

$$D^{(j)}(\mathbf{R}) T_{LM} D^{(j)\dagger}(\mathbf{R}) = \sum_{M'=-L}^L D_{M'M}^{(L)}(\mathbf{R}) T_{LM'}, \quad (3)$$

where $D_{M'M}^{(L)}(\mathbf{R})$ are the entries of the rotation matrix in the L -irrep, also called Wigner- D matrix. They also fulfill $T_{LM}^\dagger = (-1)^M T_{L-M}$. In terms of angular momentum operators J_a ($a = x, y, z$), T_{LM} 's are expressed as a sum of monomials of J_a up to degree L [33]. For example,

$$T_{10} \propto J_z, \quad T_{1\pm 1} \propto \pm J_\pm, \quad T_{20} \propto 3J_z^2 - \mathbf{J}^2. \quad (4)$$

3 Point groups of operators

In this section, we first review the Majorana representation of Hermitian operators presented in Ref. [25]

⁴ $\mathcal{B}(\mathcal{H})$ is the space of bounded operators $A : \mathcal{H} \rightarrow \mathcal{H}$ with finite Hilbert–Schmidt norm.

and explain how it can be used to associate a point group to a Hermitian operator according to its symmetries. We then generalize our approach to arbitrary non-Hermitian operators.

3.1 Majorana representation of Hermitian operators

The Majorana representation was originally introduced for pure spin states [24] (see Appendix C). It has recently been generalised to Hermitian operators in [25]. The following presentation is rather different from that of Ref. [25] but more appropriate to this work.

We start with the expansion of a general Hamiltonian in the multipolar basis,

$$H = \sum_{L=0}^{2j} \sum_{M=-L}^L h_{LM} T_{LM} \quad (5)$$

with $h_{LM} = \text{Tr}(T_{LM}^\dagger H)$ the multipolar components of H . It can be rewritten as

$$H = \sum_{L=0}^{2j} \mathbf{h}_L \cdot \mathbf{T}_L = \sum_{L=0}^{2j} h_L \hat{\mathbf{h}}_L \cdot \mathbf{T}_L, \quad (6)$$

where we gathered components with the same L into vectors $\mathbf{h}_L = (h_{LL}, \dots, h_{L-L})$ with Euclidean norm $h_L = \|\mathbf{h}_L\|_2$ and corresponding unitary vector $\hat{\mathbf{h}}_L = \mathbf{h}_L/h_L$. $\mathbf{T}_L = (T_{LL}, \dots, T_{L-L})$ is a vector whose entries are multipolar operators, and the dot product in $\mathbf{h}_L \cdot \mathbf{T}_L$ is the shorthand notation for $\sum_{M=-L}^L h_{LM} T_{LM}$. The properties of T_{LM} imply that $h_{LM}^* = (-1)^M h_{L-M}$ and that each vector \mathbf{h}_L transforms as a L -spinor under $\text{SU}(2)$ rotations⁵. Reference [25] describes how to use these properties to uniquely characterize any Hermitian operator H by

1. The Majorana representation of each constituent spinor \mathbf{h}_L , denoted $\mathfrak{C}_L(H)$ or simply \mathfrak{C}_L , which consists of a geometrical object of $2L$ points on the sphere, called a constellation of stars, with antipodal symmetry [25] (see also Appendix C). When $h_L = 0$, there is no associated constellation.
2. An equivalence class $[\mathfrak{C}_L]$ of star colorings (with two different colors available, for example black

⁵More precisely, we have from Eqs. (3) and (6)

$$D^{(j)}(\mathbf{R}) H D^{(j)\dagger}(\mathbf{R}) = \sum_{L=0}^{2j} \tilde{\mathbf{h}}_L \cdot \mathbf{T}_L$$

with $\tilde{\mathbf{h}}_L = (\tilde{h}_{LL}, \dots, \tilde{h}_{L-L})$ where

$$\tilde{h}_{LM} = \sum_{M'=-L}^L D_{MM'}^{(L)}(\mathbf{R}) h_{LM'}$$

L	\mathcal{G}	Invariant operator
1	C_∞	T_{10}
2	D_∞	T_{20}
3	C_∞	T_{30}
	D_3	$T_{33} - T_{3-3}$
	T	$T_{32} + T_{3-2}$
4	D_∞	T_{40}
	O	$T_{44} + T_{4-4} + \sqrt{\frac{14}{5}} T_{40}$
5	C_∞	T_{50}
	D_5	$T_{55} - T_{5-5}$
6	D_∞	T_{60}
	O	$T_{64} + T_{6-4} - \sqrt{\frac{2}{7}} T_{60}$
	I	$T_{65} - T_{6-5} + \sqrt{\frac{11}{7}} T_{60}$
7	C_∞	T_{70}
	D_7	$T_{77} - T_{7-7}$
	T	$T_{76} - T_{7-6} + \sqrt{\frac{13}{11}} (T_{72} - T_{7-2})$

Table 1: Examples of Hermitian operators in $\mathcal{B}^{(L)}$ exhibiting the symmetries of some point groups \mathcal{G} for $L = 1, \dots, 7$. For each L , all the indicated point groups form a set denoted $\mathcal{F}_{\max}(\mathcal{B}^{(L)})$. For example, $\mathcal{F}_{\max}(\mathcal{B}^{(4)}) = \{D_\infty, O\}$. Any operator in $\mathcal{B}^{(L)}$ necessarily has a point group equal to a subgroup of an element of $\mathcal{F}_{\max}(\mathcal{B}^{(L)})$.

and red) of \mathcal{C}_L such that each pair of antipodal stars is made up of stars of different colors. We say that two colorings belong to the same equivalence class if they differ by an even number of color exchanges in their antipodal pairs. Therefore, independently of the number and configuration of the stars, there can be only two equivalence classes for each constellation.

3. The norms h_L associated with each \mathbf{h}_L , which can be considered as the radii of the spheres of each constellation. Note that for $L = 0$, $h_0 = \text{Tr}(H)/\sqrt{2j+1}$.

In summary, $\{h_0, h_1, [\mathcal{C}_1], \dots, h_{2j}, [\mathcal{C}_{2j}]\}$ is the set of parameters required to completely and bijectively characterize a Hermitian operator (6), where \mathcal{C}_L has $2L$ stars.

3.2 Point groups of Hermitian operators via Shubnikov groups

The bijection provided by Majorana representation implies that the symmetry point group \mathcal{G}_H of a Hermitian operator H^6 is equal to the intersection of all

⁶We should formally consider the symmetry subgroups of $SU(2)$, the double cover of $SO(3)$. However, the two transformations $\pm U \in SU(2)$ that are mapped to the same rotation have the same action on any operator as $(\pm U)H(\pm U^\dagger) = UHU^\dagger$. We can therefore restrict ourselves to groups of $SO(3)$.

the point groups $\mathcal{G}_{[\mathcal{C}_L]}$:

$$\mathcal{G}_H = \bigcap_{L=1}^{2j} \mathcal{G}_{[\mathcal{C}_L]}, \quad (7)$$

where $\mathcal{G}_{[\mathcal{C}_L]} = SO(3)$ if $h_L = 0$. The possible constellations of Hermitian operators and their corresponding point groups can be studied for each subspace $\mathcal{B}^{(L)}$ separately (see Eq. (2)).

Let us now explain a systematic method to obtain the point group of an arbitrary Hermitian operator, and how to identify the largest point groups that can appear in each subspace $\mathcal{B}^{(L)}$. We begin by introducing Shubnikov groups [34] following the presentation given in [31]. Consider a set of N points on the sphere with an additional coordinate taking two possible values, for example, a color (black or red) as in our case. We now consider, besides to the usual action of $SO(3)$ on the sphere, an abstract operation I acting on the additional coordinate such that: i) I commutes with all elements of $SO(3)$, $Ig = gI$ for $g \in SO(3)$, and ii) $I^2 = E$. All products of $SO(3)$ elements and I , $\langle SO(3), I \rangle$, define a group M which, by the properties of I , reduces to [34]

$$M = SO(3) \cup I(SO(3)), \quad (8)$$

with $I(SO(3)) = \{Ig | g \in SO(3)\}$. In particular, we can choose I as the operation that switches from one equivalence class $[\mathcal{C}_L]$ to the other, *i.e.*, that exchanges the colors of the stars in one antipodal pair. At the level of operators, the action of I on $H \in \mathcal{B}^{(L)}$ would yield $-H$ [25]. Alekseĭ V. Shubnikov [34] has classified abstractly all the possible symmetry groups that a set of N points with an additional two-valued coordinate can have, which are called Shubnikov groups or magnetic point groups. Each equivalence class $[\mathcal{C}_L]$ has its corresponding Shubnikov group and proper point group, which can be calculated systematically as follows:

1. First, we consider the Majorana's constellation \mathcal{C}_L as a geometric object, without coloring, and determine its corresponding point group, denoted by $\mathcal{G}_{\mathcal{C}_L}$.
2. Then, we act with an element $g \in \mathcal{G}_{\mathcal{C}_L}$ on $[\mathcal{C}_L]$. If the equivalence class has not changed, g is a symmetry. If it has changed, g is no longer a symmetry, but Ig is. By repeating this procedure on each element of $\mathcal{G}_{\mathcal{C}_L}$, and adding I whenever necessary to obtain a symmetry operation, we get a set of elements that leave $[\mathcal{C}_L]$ invariant and form the Shubnikov point group of $[\mathcal{C}_L]$ denoted by $M_{[\mathcal{C}_L]} \subseteq M$.
3. Finally, the point group $\mathcal{G}_{[\mathcal{C}_L]}$ is the subgroup of $M_{[\mathcal{C}_L]}$ lying in $SO(3)$, $\mathcal{G}_{[\mathcal{C}_L]} = M_{[\mathcal{C}_L]} \cap \mathcal{G}_{\mathcal{C}_L}$.

At the end of the procedure, we find a group $\mathcal{G}_{[e]} \subseteq \mathcal{G}_e$ which is independent of the equivalence

j	1/2	1	3/2	2	5/2	$j \geq 3$
\mathcal{F}_{\max}	$\{C_\infty\}$	$\{D_\infty\}$	$\{D_\infty, T\}$	$\{D_\infty, O\}$	$\{D_\infty, O\}$	$\{D_\infty, O, I\}$

Table 2: Minimal sets of largest point groups $\mathcal{F}_{\max}(\mathcal{B}(\mathcal{H}^{(j)}))$ for all possible values of the spin quantum number j . These sets are valid for both Hermitian and non-Hermitian operators.

class, $\mathcal{G}_{[\mathcal{C}]} = \mathcal{G}_{[\mathcal{C}]'}$. Let us look at some examples. For the point group of a regular $2n$ -gon on a great circle, $\mathcal{G}_{[\mathcal{C}]} = D_n$. For an octahedron, $\mathcal{G}_{[\mathcal{C}]} = T$. For a cube, $\mathcal{G}_{[\mathcal{C}]} = O$. For a dodecahedron or icosahedron, $\mathcal{G}_{[\mathcal{C}]} = I$. Lastly, for a pair of n coincident points in antipodal directions, $\mathcal{G}_{[\mathcal{C}]} = C_\infty$ or D_∞ for n odd or even, respectively.

We list in Table 1 examples of Hermitian operators in $\mathcal{B}^{(L)}$ having the largest point groups for $L = 1, \dots, 7$. The same Table also shows the smallest L required for an operator to exhibit some point group symmetry.

3.3 Point groups of non-Hermitian operators

All the developments so far are valid only for Hermitian operators. However, they can be generalized to any operator S using its decomposition into a Hermitian and an anti-Hermitian component

$$S = S_H + iS_A, \quad (9)$$

where both operators $S_H = (S + S^\dagger)/2$ and $S_A = (S - S^\dagger)/2i$ are Hermitian. The decomposition is unique, and any unitary transformation applied to S preserves it by linearity. Thus, the Majorana representation of a generic operator S consists of the Majorana representation of the two parts S_H and S_A , which is again a bijective characterisation of the operator. In particular, its point group $\mathcal{G}_S = \mathcal{G}_{S_H} \cap \mathcal{G}_{S_A}$ can be calculated by using the techniques mentioned previously. A direct consequence is that the only admissible point groups of an arbitrary operator are the same point groups as for Hermitian operators or some of their subgroups. Thus, the results mentioned in Table 1 also hold for non-Hermitian operators.

3.4 Set of largest point groups and examples

Let $\mathcal{F}(V)$ be the set of point groups that can appear as the symmetry group of any element in the operator space V , excluding multiples of the identity operator. Additionally, let $\mathcal{F}_{\max}(V)$ be the minimal subset of $\mathcal{F}(V)$, such that each element of $\mathcal{F}(V)$ is a subgroup⁷ of an element of $\mathcal{F}_{\max}(V)$ ⁸.

⁷Here, we use the usual convention that a set (group) is a subset (subgroup) of itself.

⁸The set $\mathcal{F}_{\max}(V)$ can be understood as a generalization, to sets, of the concept of maximal subgroups. A proper subgroup \mathcal{G}' of a group \mathcal{G} is called *maximal* if there is no other subgroup of \mathcal{G} that contains \mathcal{G}' strictly.

The point groups listed in Table 1 correspond to $\mathcal{F}_{\max}(\mathcal{B}^{(L)})$ for $L \leq 7$. By using Eq. (7), we can now obtain $\mathcal{F}_{\max}(\mathcal{B}(\mathcal{H}^{(j)}))$ for any spin value. These sets are listed in Table 2. Since any proper point group (excluding $SO(3)$) is a subgroup of at least one of the groups D_∞, O, I , we have $\mathcal{F}_{\max}(\mathcal{B}(\mathcal{H}^{(j)})) = \mathcal{F}_{\max}(\mathcal{B}(\mathcal{H}^{(3)}))$ for $j \geq 3$. Note that the results summarized in Tables 1 and 2 are valid for both Hermitian and non-Hermitian operators. They will prove useful for the design of DD sequences.

For clarity, we show how to obtain the sets \mathcal{F} and \mathcal{F}_{\max} of $V = \mathcal{B}^{(L)}$ for $L = 1$ and 2. We consider first $L = 1$ with a generic Hamiltonian of the form $H_1 = \gamma \mathbf{J} \cdot \mathbf{n}$, where we can assume $\gamma > 0$ without loss of generality. The decomposition (6) of H_1 gives $h_0 = 0$ and $h_1 = \gamma \sqrt{j(j+1)}$, with only one constellation class $[\mathcal{C}_1]$ constituted by a pair of antipodal black and red stars (see Fig. 1, left sphere). The black (or red) star points to $\pm \mathbf{n}$, where the sign is associated with the coloring of the pair, or, in other words, with the equivalence class. It is now easy to see that $\mathcal{F}(H_1) = \mathcal{F}_{\max}(H_1) = \{C_\infty\}$.

We now turn to $L = 2$ with a generic Hamiltonian of the form $H_2 = \mathbf{h}_2 \cdot \mathbf{T}_2$. The operators of $\mathcal{B}^{(2)}$ have constellation classes $[\mathcal{C}_2]$ made up of two pairs of antipodal black and red stars (see Fig. 1, right sphere). We can identify the two black stars by the unit vectors $\{\mathbf{n}_1, \mathbf{n}_2\}$. The equivalence class $[\mathcal{C}_2]$ has two elements corresponding to constellations with black stars pointing to $\{\mathbf{n}_1, \mathbf{n}_2\}$ and $\{-\mathbf{n}_1, -\mathbf{n}_2\}$. All possible constellations can be parametrized by an angle $\delta \in [0, \pi/2]$. As an example of the procedure explained in Subsection 3.2, we consider the case where $[\mathcal{C}_2]$ forms a square on the equator ($\delta = \pi/4$). We list in Table 3 the point group of a square, which contains 8 elements. We can now determine the group $M_{[\mathcal{C}_2]}$ as explained in subsection 3.2 and shown in the second row of Table 3. From this we conclude that $\mathcal{G}_{[\mathcal{C}_2]} = D_2$. We can obtain all possible point groups for the Hermitian operators $H \in \mathcal{B}^{(L)}$ by inspecting all possible constellations $[\mathcal{C}_2]$, which yields

$$\mathcal{G}_{[\mathcal{C}_2]} = \begin{cases} D_\infty & \text{for } \delta = 0 \text{ and } \pi/2 \\ D_2 & \text{for } \delta \in (0, \pi/2) \end{cases}. \quad (10)$$

Now, the possible point groups of non-Hermitian operators $S = S_H + iS_A \in \mathcal{B}^{(2)}$, as explained in the previous subsection, are defined by the intersection of the two points groups $\mathcal{G}_{S_H} \cap \mathcal{G}_{S_A}$. The axes of symmetry of the groups may coincide or not. In particular, if $\mathcal{G}_{S_H} = \mathcal{G}_{S_A} = D_2$ and if only one axis of symmetry of each of these groups coincides, then $\mathcal{G}_{S_H} \cap \mathcal{G}_{S_A} = C_2$.

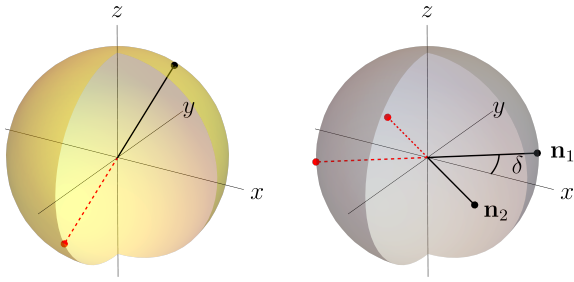


Figure 1: The constellation classes $[\mathcal{C}_1]$ (left yellow sphere) and $[\mathcal{C}_2]$ (right gray sphere) of a Hermitian operator $H \in \mathcal{B}^{(L)}$ with $L = 1, 2$. $[\mathcal{C}_2]$ is oriented so that the constellation lies in the xy -plane.

On the other hand, if they do not share any symmetry axis, then $\mathcal{G}_{S_H} \cap \mathcal{G}_{S_A} = E$. Thus, the set of point groups for generic operators (Hermitian and non-Hermitian) is $\mathcal{F}(\mathcal{B}^{(2)}) = \{E, C_2, D_2, D_\infty\}$, and $\mathcal{F}_{\max}(\mathcal{B}^{(2)}) = \{D_\infty\}$.

4 Dynamical decoupling

In this section, we recall the useful notions of dynamical decoupling at 1st order of the Magnus series.

Consider a quantum system (S) suffering from decoherence arising from unwanted interaction with an environment (bath B). The "system-bath" interaction Hamiltonian is written in Schmidt decomposition as

$$H_{SB} = \sum_{\alpha} S_{\alpha} \otimes B_{\alpha}, \quad (11)$$

where S_{α} (resp. B_{α}) are operators, not necessarily Hermitian, acting on the Hilbert space of the system (resp. of the bath). The free evolution from t_0 to t under such Hamiltonian leads to unwanted dynamics through the propagator $U_{SB}(t, t_0) = \exp(-i\Phi)$ where $\Phi \equiv (t - t_0)H_{SB}$ is called the error phase operator (EPO) [35].

To reduce this error, we can send a dynamical decoupling sequence $(-P_1 - P_2 \dots - P_N)$ that acts only on the system, which is made up of N infinitely short and strong pulses, where P_k is the unitary operator corresponding to the action of the k th pulse, and where each dash ($-$) corresponds to a free evolution of duration τ_0 , the time interval between two successive pulses. When subjected to this DD sequence, the error phase operator $\Phi = \tau_0 H_{SB}$ can be considered as undergoing the following series of unitary transformations [3, 35] in the toggling frame with respect to the DD pulses⁹,

$$\Phi \xrightarrow{-P_1} P_1^\dagger \Phi P_1 \xrightarrow{-P_2} P_1^\dagger P_2^\dagger \Phi P_2 P_1 \xrightarrow{-P_3} \dots \quad (12)$$

⁹The toggling frame corresponds here to the interaction picture with respect to the Hamiltonian implementing the pulse sequence.

where the last pulse P_N transforms the EPO back to its initial form. An average EPO over the whole sequence can then be calculated by performing a Magnus expansion in the toggling frame. This leads to $\Phi_{\text{av}} = \sum_{n=1}^{\infty} \Phi_{\text{av}}^{[n]}$ with $\Phi_{\text{av}}^{[n]}$ the n th-order term of the Magnus series, scaling as¹⁰ $\|\Phi_{\text{av}}^{[n]}\| \propto (T\|H_{SB}\|)^n$ with $T \equiv N\tau_0$ the total duration of the sequence [7]. If decoherence is small enough (*i.e.*, $T\|H_{SB}\| \ll 1$), the average EPO is well approximated by its first-order term,

$$\Phi_{\text{av}} \approx \Phi_{\text{av}}^{[1]} = \sum_{k=1}^N (g_k^\dagger \otimes \mathbb{1}_B) \Phi (g_k \otimes \mathbb{1}_B), \quad (13)$$

where we defined the propagator acting on S at each step k of the sequence as

$$g_1 \equiv \mathbb{1}_S, \quad g_k \equiv \prod_{i=1}^{k-1} P_i \quad (\text{for } 1 < k \leq N). \quad (14)$$

The products of unitary operators P_i in (14) are to be understood as being ordered chronologically, such that P_i stands to the right of P_{i+1} . Using the Schmidt decomposition (11) for Φ , we see that the DD sequence implements the following symmetrization operation on each system operator S_{α} [3, 36]

$$\Pi_{\mathcal{G}} : \mathcal{B}(\mathcal{H}_S) \rightarrow \mathcal{B}(\mathcal{H}_S) : S \mapsto \Pi_{\mathcal{G}}(S) = \frac{1}{N} \sum_{k=1}^N g_k^\dagger S g_k \quad (15)$$

where $\mathcal{G} = \{g_k\}_{k=1}^N$ denotes the set of propagators defined in Eq. (14). In the case where the set \mathcal{G} forms a group, the operator $\Pi_{\mathcal{G}}(S)$ is \mathcal{G} -invariant for any S . A similar result holds for the vector subspace spanned by the system operators $\{S_{\alpha}\}$ appearing in (11), $\mathcal{I}_S \equiv \text{span}(\{S_{\alpha}\}) \subseteq \mathcal{B}(\mathcal{H}_S)$, also called the *interaction subspace*. By linearity, $\Pi_{\mathcal{G}}(\mathcal{I}_S)$, naturally defined as the set of images of $\Pi_{\mathcal{G}}$ on every element of \mathcal{I}_S , is a vector subspace that contains only \mathcal{G} -invariant operators. By choosing a group \mathcal{G} such that $\Pi_{\mathcal{G}}(\mathcal{I}_S) = \text{span}(\{\mathbb{1}_S\})$, called a *decoupling group* of \mathcal{I}_S [4, 37], we ensure that

$$\Phi_{\text{av}}^{[1]} \propto \mathbb{1}_S \otimes B, \quad (16)$$

where B is some operator acting on the bath Hilbert space. Thereby, the undesirable dynamics caused by the interaction with the bath is eliminated at the dominant order of the Magnus series. Any decoupling group \mathcal{G} has its corresponding *correctable subspace* $\mathcal{C}_{\mathcal{G}} \subseteq \mathcal{B}(\mathcal{H}_S)$ [37], defined as the subspace that contains all the operators in $\mathcal{B}(\mathcal{H}_S)$ for which their image of $\Pi_{\mathcal{G}}$ are proportional to the identity¹¹.

¹⁰ $\|A\|$ denotes here the supremum operator norm of A defined as $\|A\| = \sup_{|\psi\rangle \in \mathcal{H}_S} \frac{\|A|\psi\rangle\|}{\| |\psi\rangle \|}$.

¹¹Formally speaking, the correctable subspace is defined as the pre-image $\mathcal{C}_{\mathcal{G}} = \Pi_{\mathcal{G}}^{-1}(\text{span}(\{\mathbb{1}_S\}))$, which is a vector space.

$$\begin{array}{c|cccccccc} \mathcal{G}_{\mathcal{C}_2} & E & R(\mathbf{z}, \pi/2) & R(\mathbf{z}, \pi) & R(\mathbf{z}, 3\pi/2) & R(\mathbf{x}, \pi) & R(\mathbf{y}, \pi) & R(\mathbf{n}_1, \pi) & R(\mathbf{n}_2, \pi) \\ \hline M_{[\mathcal{C}_2]} & E & IR(\mathbf{z}, \pi/2) & R(\mathbf{z}, \pi) & IR(\mathbf{z}, 3\pi/2) & R(\mathbf{x}, \pi) & R(\mathbf{y}, \pi) & IR(\mathbf{n}_1, \pi) & IR(\mathbf{n}_2, \pi) \end{array},$$

Table 3: Elements of the groups associated with the constellation \mathcal{C}_2 shown in Fig. 1 (right sphere) with $\delta = \pi/4$. The elements of $\mathcal{G}_{\mathcal{C}_2}$ leave the constellation invariant if we ignore the color of the stars, whereas the elements of $M_{[\mathcal{C}_2]}$ leave the constellation invariant when we take the color of the stars into account. The point group of the equivalence class $[\mathcal{C}_2]$ is the intersection of the two sets, *i.e.*, $\mathcal{G}_{[\mathcal{C}_2]} = \{E, R(\mathbf{z}, \pi), R(\mathbf{x}, \pi), R(\mathbf{y}, \pi)\} = D_2$.

In particular, we call a group \mathcal{G}_{uni} a *universal decoupling group* if its correctable subspace contains the entire Hilbert-Schmidt space of system operators, *i.e.*, $\mathcal{C}_{\mathcal{G}_{\text{uni}}} = \mathcal{B}(\mathcal{H}_S)$.

Thus, to achieve first-order decoupling for a given Hamiltonian (11), we should choose \mathcal{G} such that $\mathcal{I}_S \subseteq \mathcal{C}_{\mathcal{G}}$. From this decoupling group \mathcal{G} , it is then possible to systematically construct a pulse sequence satisfying Eq. (14) by choosing a generating set $\Gamma \subseteq \mathcal{G}$, drawing the Cayley graph with respect to this set of generators and finally finding a cycle on the graph that visits each vertex the same number of times [4, 38]. Different paths can lead to different decoupling properties; in particular, a Hamiltonian path (which visits each vertex exactly once) corresponds to the smallest sequence of pulses that implements the decoupling operation, while an Eulerian path (which visits each edge exactly once) naturally possesses a certain robustness to finite-duration errors [4]. Adding further edges and loops to the path on the graph, corresponding to additional accessible pulses, can also enable the construction of more efficient sequences [7]. More information on Cayley graphs in the context of dynamical decoupling can be found in Appendix B.

In this work, we focus on decoupling groups associated with proper point groups, *i.e.*, decoupling groups constructed solely from $SU(2)$ operations. Using the formalism described in Sec. 3, we can find out, for a given system-bath interaction Hamiltonian and its respective interaction subspace \mathcal{I}_S , the rotation symmetries that are impossible for any operator $S \in \mathcal{I}_S \setminus \text{span}(\{\mathbb{1}_S\})$. The corresponding inaccessible point groups are then decoupling groups, as we explain below. Using this strategy, we identify and study decoupling groups for a wide range of individual and multipartite quantum systems.

5 Decoupling groups for single spins

In this section, we develop a general framework for selecting decoupling groups of a single spin- j according to its interaction subspace. The general theory is summarized in Proposition 1 and Table 4 and is applied to several systems.

5.1 General theory

Consider a single spin- j system, with Hilbert space $\mathcal{H}_S = \mathcal{H}^{(j)}$, interacting with its environment via the

interaction Hamiltonian (11), leading to the interaction subspace $\mathcal{I}_S = \text{span}(\{S_\alpha\})$. The subspace \mathcal{I}_S , which may not be closed under $SU(2)$ operations, is contained in a direct sum of irreps

$$\mathcal{I}_S \subseteq \bigoplus_{L=0}^{L_{\max}} \mathcal{B}^{(L)} \subseteq \mathcal{B}(\mathcal{H}_S) \quad (17)$$

where $L_{\max} \leq 2j$ is the smallest L value for which the first inclusion is valid, and where the irrep $\mathcal{B}^{(0)}$ (0-irrep) contains only operators proportional to the identity $\mathbb{1}_S$. For any point group \mathcal{G} , the symmetrization operation $\Pi_{\mathcal{G}}$ defined in Eq. (15) maps any element of an L -irrep $\mathcal{B}^{(L)}$ to a \mathcal{G} -invariant element of the same irrep. Thus, \mathcal{I}_S remains, after symmetrization, contained in the same direct sum of irreps

$$\Pi_{\mathcal{G}}(\mathcal{I}_S) \subseteq \bigoplus_{L=0}^{L_{\max}} \mathcal{B}^{(L)}. \quad (18)$$

This latter result combined with (7) and (9) implies that the symmetry groups of the operators in \mathcal{I}_S (except the identity) after symmetrization fulfill

$$\mathcal{F}(\Pi_{\mathcal{G}}(\mathcal{I}_S)) \subseteq \mathcal{F}\left(\bigoplus_{L=0}^{L_{\max}} \mathcal{B}^{(L)}\right), \quad (19)$$

where the set on the r.h.s. of (19) can be determined based only on the Tables 1 and 4. In particular, if a group $\mathcal{G}' \notin \mathcal{F}_{\max}\left(\bigoplus_{L=0}^{L_{\max}} \mathcal{B}^{(L)}\right)$, then $\mathcal{G}' \notin \mathcal{F}_{\max}(\Pi_{\mathcal{G}}(\mathcal{I}_S))$, which means that $\Pi_{\mathcal{G}'}(\mathcal{I}_S) = \text{span}(\{\mathbb{1}_S\})$ because (i) $\Pi_{\mathcal{G}'}(\mathcal{I}_S)$ has no \mathcal{G}' -invariant operator but those proportional to the identity and (ii) $\Pi_{\mathcal{G}'}(\mathcal{I}_S)$ is a \mathcal{G}' -invariant subspace. In other words, \mathcal{G}' is a decoupling group for \mathcal{I}_S . We merge all these observations into the following proposition.

Proposition 1. *Consider a single quantum system of spin j interacting with its environment, whose interaction subspace $\mathcal{I}_S \subseteq \bigoplus_{L=0}^{L_{\max}} \mathcal{B}^{(L)}$ for some integer $L_{\max} \geq 1$. Any point group that is not a subgroup of an element of $\mathcal{F}_{\max}\left(\bigoplus_{L=0}^{L_{\max}} \mathcal{B}^{(L)}\right)$ is a decoupling group of \mathcal{I}_S . For $L_{\max} = 2j$, this is a universal decoupling group.*

Note that Proposition 1 refers to a subgroup (not a proper subgroup), which may be the group itself. The smallest decoupling groups for the first values of L_{\max} are listed in Table 4, derived from the results contained in Tables 1 and 2. The following corollaries follow.

L_{\max}	\mathcal{G}	$ \mathcal{G} $
1	2-Dihedral (D_2)	4
2	Tetrahedral (T)	12
3	Octahedral (O)	24
4 or 5	Icosahedral (I)	60

Table 4: Smallest decoupling point groups for any interaction subspace $\mathcal{I}_S \subseteq \bigoplus_{L=0}^{L_{\max}} \mathcal{B}^{(L)}$ for different values of L_{\max} , and their cardinality. For $L_{\max} \geq 6$, there is no decoupling group composed solely of rotations. The point groups listed are universal decoupling groups for single spin systems with spin quantum number $j \leq L_{\max}/2$.

Corollary 1. *There is no universal decoupling group based solely on rotations when $j \geq 3$.*

Corollary 2. *If the interaction subspace contains an entire irrep with $L \geq 6$, then there is no decoupling group based solely on rotations.*

5.2 Applications

We are now in a position to construct a sequence of pulses for each decoupling group of Table 4 by choosing an Eulerian path on the corresponding Cayley graph. In particular, each group appearing in Table 4, and thus its corresponding Cayley graph, has two generators (a, b) . The exact form of the resulting sequences and details of their construction can be found in Appendix B, but the results are summarized in Table 5. For the most elementary system, the qubit (spin-1/2), the smallest universal decoupling group is D_2 . The corresponding Eulerian sequence has already been used in the literature and has been called *Eulerian Dynamical Decoupling* (EDD) [4]. The novelty here lies in the three other exceptional groups appearing in Table 4. We call their Eulerian sequences *Platonic DD sequences* because their respective symmetries are the same as those of Platonic solids. We denote them by XEDD, with $X \in \{T, O, I\}$.

A direct application of our framework is the construction of universal decoupling groups for a single spin j (using Proposition 1 with $L_{\max} = 2j$). For spins with $j < 3$, it is possible to find a universal decoupling group in Table 4 since it suffices to choose any of the decoupling groups with $L_{\max} \geq 2j$. For example, the octahedral group is a universal decoupling group for spins 1/2, 1 and 3/2.

To demonstrate and validate the decoupling properties of the Platonic sequences, we use the DD performance quantifier introduced in Ref. [7] and defined as

$$D(\mathbb{1}_S, U_S) = \sqrt{1 - \frac{|\text{Tr}[U_S]|}{2j+1}}. \quad (20)$$

This quantifier D was derived in Ref. [39] and is a distance measure between the identity operator $\mathbb{1}_S$ (the

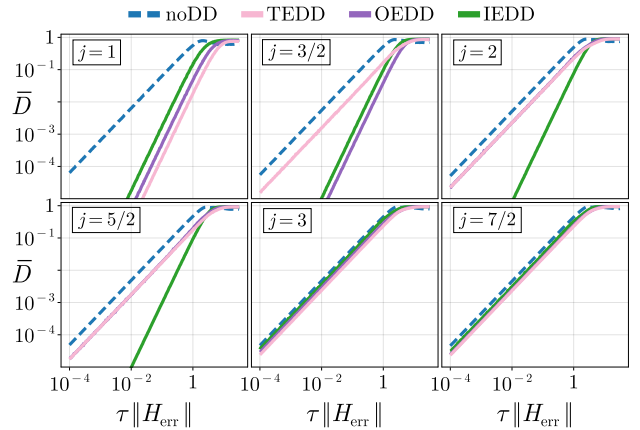


Figure 2: Average distance \bar{D} between the identity propagator and the noisy propagator for a single spin- j system (where j ranges from 1 to $7/2$), with and without DD sequence. \bar{D} is plotted as a function of $\tau \|H_{\text{err}}\|$ for the TEDD (purple), OEDD (red) and IEDD (green) sequences and for the free evolution (noDD, blue). H_{err} is a Hermitian error Hamiltonian and τ is the total time of the free propagation (and also the duration of the TEDD sequence, see main text).

desired free evolution operator) and a noisy propagator U_S . The smaller D is, the more freely the system evolves without perturbation, and the better the DD sequence. Here, we consider a noisy propagator $U_S = \exp(-iH_{\text{err}}\tau)$ generated by a random error Hamiltonian H_{err} drawn from the Gaussian ensemble of random $(2j+1) \times (2j+1)$ Hermitian matrices. Figure 2 shows the average distance $\bar{D}(\mathbb{1}_S, U_S)$ as a function of $\tau \|H_{\text{err}}\|$ in log-log scale for the free evolution (*i.e.*, without the DD sequence) and with the application of each of the Platonic sequences. The average was computed over 5000 random Hamiltonians. The time τ is the duration of both the total free evolution and the shortest sequence (TEDD in this case). To enable a fair comparison of performance between the different sequences, the time interval between successive pulses was chosen to be identical for each sequence.

When there is no first-order decoupling, the average distance \bar{D} should scale as $\bar{D} \propto \tau \|H_{\text{err}}\|$, according to the Magnus expansion. This is indeed the behavior we observe, for any spin, in the log-log plot in Fig. 2 in the absence of DD sequence (dashed blue curves with a slope of 1) and for certain DD sequences. In this plot, a slope that is twice as steep indicates first-order decoupling, *i.e.*, $\bar{D} \propto (\tau \|H_{\text{err}}\|)^2$ [7]. It can also be seen that when several sequences achieve decoupling, those with a smaller decoupling group result in a smaller distance and therefore better performance. This can be understood by the fact that the time required to implement a DD sequence is proportional to the order of the decoupling group.

Although platonic sequences do not achieve full decoupling for $j \geq 3$, they can nevertheless be of great practical interest for dynamical decoupling of large

Decoupling group	Platonic sequence	Generators		# pulses	Sequence
		a	b		
2-Dihedral (D_2)	EDD	$((1, 0, 0), \pi)$	$((0, 1, 0), \pi)$	8	$abab^2aba$
Tetrahedral (T)	TEDD	$((0, 0, 1), \frac{2\pi}{3})$	$((\frac{\sqrt{2}}{3}, \sqrt{\frac{2}{3}}, \frac{1}{3}), \frac{2\pi}{3})$	24	$aba^2bab^3a^2bab^3a^2bab^2a^2$
Octahedral (O)	OEDD	$((0, 0, 1), \frac{2\pi}{4})$	$(\frac{1}{\sqrt{3}}(1, 1, 1), \frac{2\pi}{3})$	48	see Appendix B, Eq. (68)
Icosahedral (I)	IEDD	$(\frac{(0, -1, \phi)}{\sqrt{\phi+2}}, \frac{2\pi}{5})$	$(\frac{(1-\phi, 0, \phi)}{\sqrt{3}}, \frac{2\pi}{3})$	120	see Appendix B, Eq. (69)

Table 5: Summary of the Platonic DD sequences constructed from the point groups T, O and I. The generators are specified in the axis-angle notation and correspond to the two types of pulses required to implement each sequence. The two shortest sequences are given in their condensed notation and we refer to Appendix B for the two longest sequences. In the IEDD sequence generators, $\phi = \frac{\sqrt{5}+1}{2}$ is the golden ratio.

spins [40, 41]. Indeed, the TEDD sequence is capable of decoupling any Hamiltonian with $\mathcal{I}_S \subseteq \bigoplus_{L=1}^2 \mathcal{B}^{(L)}$, regardless the spin j of the system. In this case, \mathcal{I}_S consists of linear combinations of operators that are linear or quadratic with respect to the angular momentum operators. The EDD sequence, in contrast, only handles terms linear in the spin operators. As an example, we compare the performance of the EDD and TEDD sequences for a spin-1 on random error Hamiltonians of the form $H^{(1)} = \sum_{L=0}^2 \mathbf{h}_L \cdot \mathbf{T}_L$. The average distance \bar{D} is shown in the $(\tau h_1, \tau h_2)$ parameter space in Fig. 3; when $h_1/h_2 \ll 1$ (resp. $h_1/h_2 \gg 1$), the distance scales as $\bar{D} \propto (\tau h_2)^r$ (resp. $\bar{D} \propto (\tau h_1)^r$) with $r = 1$ when there is no decoupling and $r = 2$ when first-order decoupling is achieved. As expected, we observe that the TEDD sequence outperforms the EDD sequence in cases where the quadratic components h_2 are not negligible compared to the linear components ($r = 2$ for TEDD and $r = 1$ for EDD in the regime $h_1/h_2 \ll 1$). A similar advantage of the OEDD sequence over the TEDD sequence is observed in Fig. 4 for random spin-3/2 Hamiltonians of the form $H^{(3/2)} = \sum_{L=2}^3 \mathbf{h}_L \cdot \mathbf{T}_L$, where we show the average distance in the parameter space $(\tau h_2, \tau h_3)$. Here we set h_0 and h_1 equal to zero for convenience. To close this section on individual spins, it should be noted that similar results can be obtained for any spin, since the decoupling properties of the sequences depend only on L_{\max} and not on j .

6 Decoupling spin-spin interactions with global rotations

We will now extend the framework of Sec. 5 to multi-spin systems where we seek to decouple the environment and/or some spin-spin interactions by using pulses composed only of global SU(2) transformations, *i.e.*, the same SU(2) operation is applied to each spin. Our main theoretical results are summarized in Proposition 2 and in Table 6, then applied to several systems. As explained below, some spin interactions cannot be decoupled using only global ro-

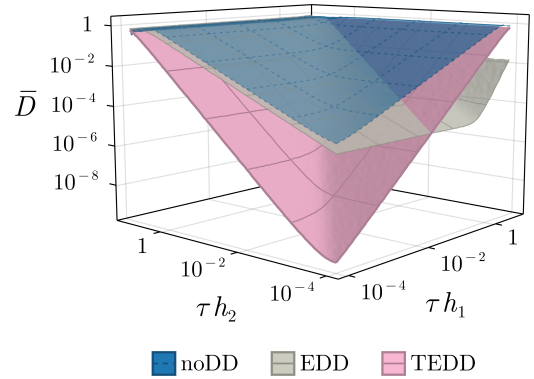


Figure 3: Average distance \bar{D} between the identity propagator and the noisy propagator in the $(\tau h_1, \tau h_2)$ parameter space for a single spin-1 system, for the free evolution (blue) and the EDD (gray) and TEDD (pink) sequences. The averages were performed over 1000 randomly generated Hamiltonians.

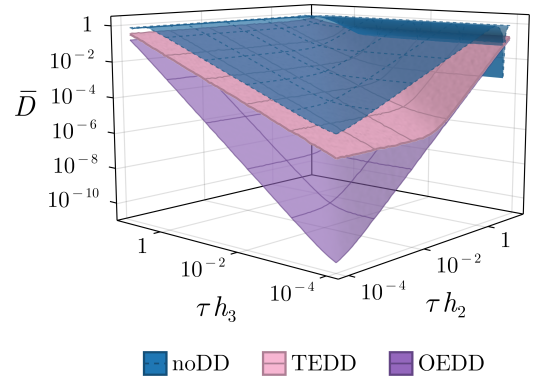


Figure 4: Same as in Fig. 3 but in the $(\tau h_2, \tau h_3)$ parameter space of a single spin-3/2 system, for the free evolution (blue) and the TEDD (pink) and OEDD (purple) sequences. The averages were performed over 1000 randomly generated Hamiltonians.

tations; these are identified and listed in Appendix E for the first nontrivial systems.

6.1 General theory

Consider an ensemble of N interacting spins (system S), of spin quantum numbers j_k ($k = 1, \dots, N$), coupled to an environment (bath B). Depending on the interactions we want to decouple, the Hamiltonian H will include interactions between the system and the bath, interactions between the spins, or both. The Schmidt decomposition of H with respect to the bipartition of spin k and its complement is as follows

$$H = \sum_{\alpha} S_{\alpha}^k \otimes C_{\alpha}^k \quad (21)$$

where the C_{α}^k are operators acting on the Hilbert space of the spins and/or the bath, depending on the case. The interaction subspace for spin k is thus given by $\mathcal{I}_S^k = \text{span}(\{S_{\alpha}^k\}_{\alpha})$. We can now define the interaction subspace of the system, \mathcal{I}_S , as the tensor product of the individual interaction subspaces

$$\mathcal{I}_S = \bigotimes_{k=1}^N \mathcal{I}_S^k, \quad \text{with} \quad \mathcal{I}_S^k \subseteq \bigoplus_{L_k=0}^{L_{\max}^k} \mathcal{B}_{j_k}^{(L_k)}. \quad (22)$$

From Eq. (22), we have that \mathcal{I}_S is contained in a direct sum of irreps

$$\begin{aligned} \mathcal{I}_S &\subseteq \bigotimes_{k=1}^N \left(\bigoplus_{L_k=0}^{L_{\max}^k} \mathcal{B}_{j_k}^{(L_k)} \right) = \bigoplus_{L_1=0}^{L_{\max}^1} \cdots \bigoplus_{L_N=0}^{L_{\max}^N} \left(\bigotimes_{k=1}^N \mathcal{B}_{j_k}^{(L_k)} \right) \\ &= \bigoplus_{\mathbf{L}} \left(\bigotimes_{k=1}^N \mathcal{B}_{j_k}^{(L_k)} \right), \end{aligned} \quad (23)$$

with $\mathbf{L} \equiv (L_1, \dots, L_N)$ a vector-index, where L_k runs from 0 to $L_{\max}^k \leq 2j_k$. The possible interaction operators of \mathcal{I}_S can be grouped into K -body terms (with $K = 0, \dots, N$ ¹²) according to the number of zero components in each index \mathbf{L} of the direct sum. More specifically, when \mathbf{L} has exactly $N - K$ zero components, an operator in $\bigotimes_{k=1}^N \mathcal{B}_{j_k}^{(L_k)}$ has only K -body terms. Note that 1-body terms correspond to 1-local Hamiltonians and 0-body terms to operators proportional to the global identity. For each \mathbf{L} , the corresponding subspace decomposes entirely into irreps as follows

$$\bigotimes_{k=1}^N \mathcal{B}_{j_k}^{(L_k)} = \bigoplus_{(\tilde{L}, \alpha)} \tilde{\mathcal{B}}^{(\tilde{L}, \alpha)}, \quad (24)$$

where $\tilde{L} \in \{\tilde{L}_{\min}, \tilde{L}_{\min} + 1, \dots, \tilde{L}_{\max}\}$, with $\tilde{L}_{\min} = \min_{\mathbf{n} \in \{0,1\}^N} \left(\left| \sum_{k=1}^N (-1)^{n_k} L_k \right| \right)$ and $\tilde{L}_{\max} = \sum_{k=1}^N L_k$ according to the angular momenta coupling rules [33, 42]. Different subspaces with the same value of \tilde{L} may appear, hence the use of the subscript α to distinguish them. The irreps decomposition for

¹²When $K \geq 2$, we call the K -body terms also K -body interactions.

each \mathbf{L} with K -body terms is independent and none of them contains the global identity, except for $\mathbf{L} = \mathbf{0}$ ($K = 0$). The interaction subspace \mathcal{I}_S can thus be contained in a minimal direct sum of irreps

$$\mathcal{I}_S \subseteq \bigoplus_{\mathbf{L}} \bigoplus_{(\tilde{L}, \alpha_{\mathbf{L}})} \tilde{\mathcal{B}}^{(\tilde{L}, \alpha_{\mathbf{L}})} \quad (25)$$

Crucially, for a group \mathcal{G} composed of global rotations, the symmetrization operation (15) does not couple different irreps, so again we have

$$\Pi_{\mathcal{G}}(\mathcal{I}_S) \subseteq \bigoplus_{\mathbf{L}} \bigoplus_{(\tilde{L}, \alpha_{\mathbf{L}})} \tilde{\mathcal{B}}^{(\tilde{L}, \alpha_{\mathbf{L}})} \quad (26)$$

and

$$\mathcal{F}(\Pi_{\mathcal{G}}(\mathcal{I}_S)) \subseteq \mathcal{F} \left(\bigoplus_{\mathbf{L}} \bigoplus_{(\tilde{L}, \alpha_{\mathbf{L}})} \tilde{\mathcal{B}}^{(\tilde{L}, \alpha_{\mathbf{L}})} \right). \quad (27)$$

The largest irrep appearing in the decomposition (25) has an effective angular momentum j_{eff} equal to half the sum of the K largest L_{\max}^k 's. Thus, the set of decoupling groups of N interacting spins with up to K -body terms is the same set as for a single spin j_{eff} ; a case already examined in the previous section. Consequently, we can use the results presented in Tables 1 and 2 to find decoupling groups for different types of spin interactions. However, it is essential to note that the r.h.s. of Eq. (25) may have 0-irreps for $\mathbf{L} \neq \mathbf{0}$ which do not correspond to the global identity operator. Instead, they correspond to other SU(2) invariant subspaces whose operators cannot be averaged to zero by global SU(2) operations. In particular, they are insensitive to the DD sequences studied in this work. Some examples of such isotropic operators are $\mathbf{J}^1 \cdot \mathbf{J}^2$ and $\mathbf{J}^1 \cdot (\mathbf{J}^2 \times \mathbf{J}^3)$. The conditions that guarantee the absence of isotropic components in a Hamiltonian, which we call *anisotropy conditions*, are derived and discussed in Appendix E for: 1) multilinear K -body terms¹³ for $N = 2, 3, 4$, and 2) for an arbitrary system with at most two-body terms.

The general result described above is formulated as follows:

Proposition 2. *Consider an ensemble of N spins j_k ($k = 1, \dots, N$) with a Hamiltonian with at most K -body terms and such that its interaction subspace (22) contains no 0-irreps (isotropic components) except the global identity. Any group that is not a subgroup of $\mathcal{F}_{\max}(\mathcal{B}(\mathcal{H}^{(j_{\text{eff}})}))$, where j_{eff} is half the sum of the K largest L_{\max}^k 's, is then a decoupling group for \mathcal{I}_S .*

¹³A *multilinear* K -body term means that $L_{\max}^k = 1$ for exactly K different values of k and $L_{\max}^k = 0$ for the other values of k , i.e., the interactions consist of a linear combination of tensor products of K operators proportional to the angular momentum operators J_a^k where $a = x, y, z$ and k is the spin label.

(a)		K				
L_{\max}		2	3	4	5	≥ 6
1		T	O	I	I	–
2		I	–	–	–	–
≥ 3		–	–	–	–	–

(b)		L_{\max}^2				
L_{\max}^1		1	2	3	4	≥ 5
1		T	O	I	I	–
2			I	I	–	–
3				–	–	–
4					–	–

Table 6: (a) Decoupling groups for an ensemble of spins, with quantum numbers j_k and interaction subspace $\mathcal{I}_S^k \subseteq \bigoplus_{L=0}^{L_{\max}} \mathcal{B}^{(L)}$, with at most K -body terms. (b) Decoupling groups for two-body interactions for different values of $L_{\max}^1 \leq L_{\max}^2$. In both cases, we assume that the anisotropy conditions are fulfilled, so that the Hamiltonian does not contain isotropic components.

The smallest decoupling groups for up to K -body terms where the interaction subspace of each constituent has the same $L_{\max}^k = L_{\max}$ are listed in Table 6a for different values of K and L_{\max} . The smallest decoupling groups for two-body interactions are listed in Table 6b for different pairs (L_{\max}^1, L_{\max}^2) .

6.2 Applications

Proposition 2 allows us to obtain decoupling groups for certain multispin systems with K -body terms, which we present in Table 6a. For example, we find that the group T (resp. O) is a decoupling group for any spin ensemble with only two-body (resp. two- and three-body) multilinear interaction terms, provided that the Hamiltonian satisfies the anisotropy conditions. For two-body and three-body interactions, this means ensuring that the Hamiltonian has no isotropic components, which are of the form (see Appendix E)

$$\begin{aligned} H_{\text{isotropic}}^{\text{two-body}} &\propto \mathbf{J}^1 \cdot \mathbf{J}^2, \\ H_{\text{isotropic}}^{\text{three-body}} &\propto \mathbf{J}^1 \cdot (\mathbf{J}^2 \times \mathbf{J}^3). \end{aligned} \quad (28)$$

Thus, the anisotropy conditions for the most general Hamiltonian with multilinear two- and three-body interactions, written as

$$\begin{aligned} H = & \underbrace{\sum_{i < j} \sum_{\alpha, \mu} h_{\alpha\mu}^{ij} J_{\alpha}^i \otimes J_{\mu}^j}_{\equiv H^{\text{two-body}}} \\ & + \underbrace{\sum_{i < j < k} \sum_{\alpha, \mu, \lambda} h_{\alpha\mu\lambda}^{ijk} J_{\alpha}^i \otimes J_{\mu}^j \otimes J_{\lambda}^k}_{\equiv H^{\text{three-body}}}, \end{aligned} \quad (29)$$

are

Two-body anisotropy conditions:

$$\sum_{\alpha, \beta} h_{\alpha\beta}^{ij} \delta_{\alpha\beta} = 0, \quad \forall i \neq j \quad (30)$$

Three-body anisotropy conditions:

$$\sum_{\alpha, \beta, \lambda} h_{\alpha\beta\lambda}^{ijk} \epsilon_{\alpha\beta\lambda} = 0, \quad \forall i \neq j \neq k \neq i. \quad (31)$$

To illustrate the decoupling properties of Platonic sequences on multispin systems, we again compute the average distance \bar{D} , this time for an ensemble of four spin-1/2 with interaction Hamiltonian of the form (29), for the free evolution and with the application of the OEDD and TEDD sequences. Figure 5 shows the distance in the $(\tau\beta, \tau\Lambda)$ parameter space, where β and Λ are defined as

$$\beta = \|H^{\text{two-body}}\|, \quad \Lambda = \|H^{\text{three-body}}\|. \quad (32)$$

The tensors h^{ij} and h^{ijk} appearing in the Hamiltonian (29) are randomly generated so as to satisfy the anisotropy conditions (30) and (31). The decoupling properties of the T and O groups for multiqubit interactions can be read in Fig. 5 by the slope of \bar{D} as a function of $\tau\beta$ for $\tau\Lambda \ll 1$, and as a function of $\tau\Lambda$ for $\tau\beta \ll 1$. The TEDD and OEDD sequences both provide first-order decoupling for dominating two-body multilinear interactions ($\Lambda \ll \beta$), while the OEDD sequence is the only one to also provide first-order decoupling for dominating three-body multilinear interactions ($\Lambda \gg \beta$). Numerical calculations (data not shown) confirm that first-order decoupling is not achieved when the conditions (31) are not satisfied. Table 6a also shows that no decoupling group (consisting only of global rotations) exists for interactions involving simultaneously 6 or more bodies in an ensemble of interacting qubits.

On the other hand, Table 6b shows the decoupling groups for two-body interactions of a composite system. Without loss of generality, we can assume a bipartite system. As an example, we consider a qubit-qutrit system, which is equivalent to a two spin system with $j = 1/2$ and 1. Its most general Hamiltonian can be expanded as

$$H = \sum_{L_1=0}^1 \sum_{L_2=0}^2 \sum_{M_1=-L_1}^{L_1} \sum_{M_2=-L_2}^{L_2} w_{M_1 M_2}^{L_1 L_2} T_{L_1 M_1} \otimes T_{L_2 M_2} \quad (33)$$

where the tensors $w^{L_1 L_2}$ should satisfy the hermiticity conditions

$$w_{-M_1 - M_2}^{L_1 L_2} = (-1)^{M_1 + M_2} \left(w_{M_1 M_2}^{L_1 L_2} \right)^* \quad (34)$$

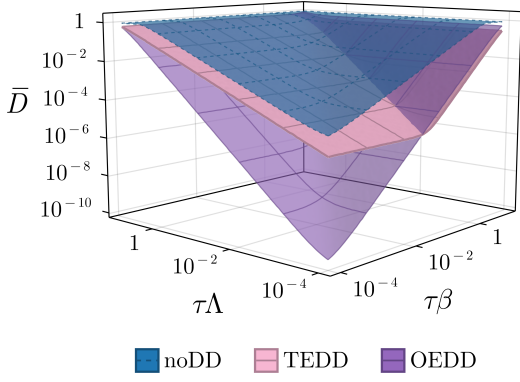


Figure 5: Average distance \bar{D} between the identity propagator and the noisy propagator in the $(\tau\beta, \tau\Lambda)$ parameter space for an ensemble of four interacting spin-1/2 with two and three-body interactions, for the free evolution (blue) and the TEDD (pink) and OEDD (purple) sequences. Averages were performed on 1000 randomly generated Hamiltonian satisfying the anisotropy conditions (30) and (31).

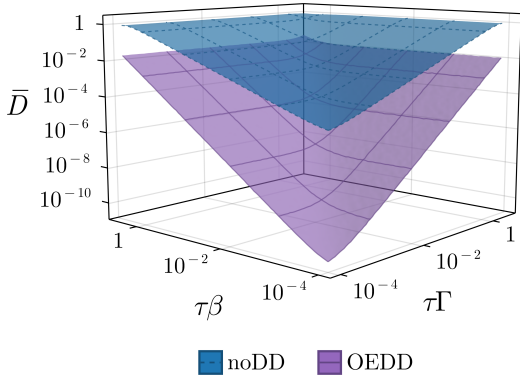


Figure 6: Same as in Fig. 5 in the $(\tau\Gamma, \tau\beta)$ parameter space for the free evolution (blue) and the OEDD sequence (purple) for a qubit-qudit composite spin system.

The SU(2) isotropic component of (33) is necessarily of the form (see Appendix E)

$$H_{\text{isotropic}}^{\text{two-body}} \propto \sum_{M=-1}^1 (-1)^M T_{1M} \otimes T_{1-M} \quad (35)$$

$$\propto \mathbf{J}^{\text{qubit}} \cdot \mathbf{J}^{\text{qudit}}$$

The anisotropy condition on the Hamiltonian will therefore be equivalent to the condition (30). Defining Γ (resp. β) as the supremum operator norm of the one-body (resp. two-body) Hamiltonian, we compare in Fig. 6 the OEDD sequence with the free evolution in the $(\tau\Gamma, \tau\beta)$ parameter space, where τ is the duration of the free evolution and the pulse sequence. Once again, we observe the first-order decoupling obtained with the OEDD sequence through the slope of \bar{D} as a function of $\tau\Gamma$ and $\tau\beta$.

7 Robustness to control errors and finite pulse duration errors

So far, we have considered infinitely short and strong DD pulses, without imperfections due to control errors. However, in a realistic setting, the pulses take some time to implement (a time during which decoherence occurs) and may not be perfect; consequently, the resulting decoupling may also not be perfect. We therefore carry out a robustness analysis of the Platonic sequences in this section.

Consider a dynamical decoupling sequence designed from a certain group \mathcal{G} (of correctable subspace $\mathcal{C}_{\mathcal{G}}$) with certain generators $\{P_{\lambda}\}$, where each pulse $P \in \{P_{\lambda}\}$ has a certain finite duration $\tau_P \in \{\tau_{P_{\lambda}}\}$. Assume, without loss of generality, that there is no free evolution between the pulses *i.e.*, once a pulse is completed, the next one starts¹⁴. During the implementation of each pulse, three Hamiltonians contribute to the dynamics, namely (i) the ideal pulse Hamiltonian $H_P(t) \in \mathcal{B}(\mathcal{H}_S)$, (ii) the pulse error Hamiltonian $H_P^{\text{err}}(t) \in \mathcal{B}(\mathcal{H}_S)$, and (iii) the decoherence Hamiltonian $H_{SB} = \sum_{\alpha} S_{\alpha} \otimes B_{\alpha} \in \mathcal{B}(\mathcal{H}_{SB})$, from which the interaction subspace \mathcal{I}_S is usually defined. The pulse error and decoherence Hamiltonians will cause the pulse to slightly deviate from the intended unitary; this deviation can be quantified by an EPO Φ_P by moving to the toggling frame with respect to $H_P(t)$. The EPO is defined by the following equation

$$e^{-i\Phi_P} \equiv \mathcal{T} \exp \left\{ -i \int_0^{\tau_P} \left[\sum_{\alpha} P^{\dagger}(t) S_{\alpha} P(t) \otimes B_{\alpha} + P^{\dagger}(t) H_P^{\text{err}}(t) P(t) \otimes \mathbf{1}_B \right] dt \right\}, \quad (36)$$

where $P(t)$ is the propagator associated with $H_P(t)$, with $P(\tau_P) = P$, and \mathcal{T} is the time-ordering operator. The exact form of the EPO can be formally calculated by performing a Magnus expansion; when both the decoherence and the pulse errors are small enough, it is well approximated by its first-order contribution, *i.e.*,

$$\Phi_P \approx \Phi_P^{[1]} = \sum_{\alpha} F_{(P, \tau_P)}[S_{\alpha}] \otimes B_{\alpha} + F_{(P, \tau_P)}[H_P^{\text{err}}(t)] \otimes \mathbf{1}_B, \quad (37)$$

where we define the function $F_{(P, \tau_P)}[\cdot] : \mathcal{B}(\mathcal{H}_S) \rightarrow \mathcal{B}(\mathcal{H}_S)$ as

$$F_{(P, \tau_P)}[S] = \int_0^{\tau_P} P^{\dagger}(t) S P(t) dt. \quad (38)$$

A key result of Ref. [4] is that if we choose an Eulerian sequence and if the errors $H_P^{\text{err}}(t)$ are systematic,

¹⁴Since no assumptions are made about the shape of the pulses, we can always add a free evolution time by simply turning off the control Hamiltonian for a certain period of time.

i.e., the same error Hamiltonian $H_P^{\text{err}}(t)$ occurs each time $H_P(t)$ is turned on, the first-order EPO of the total sequence is given by

$$\Phi_{\text{EDD}}^{[1]} = \sum_{\lambda} \left\{ \sum_{\alpha} \Pi_G \left[F_{(P_{\lambda}, \tau_{P_{\lambda}})} [S_{\alpha}] \right] \otimes B_{\alpha} + \Pi_G \left[F_{(P_{\lambda}, \tau_{P_{\lambda}})} [H_{P_{\lambda}}^{\text{err}}] \right] \otimes \mathbb{1}_B \right\}, \quad (39)$$

and $\Phi_{\text{EDD}} \approx \Phi_{\text{EDD}}^{[1]}$ if decoherence is small enough. We can now define the subspace $\mathcal{I}_{P_{\lambda}}$ as the subspace spanned by the pulse error Hamiltonian at different times,

$$\mathcal{I}_{P_{\lambda}} \equiv \text{span}(H_{P_{\lambda}}^{\text{err}}(t) \forall t) \quad (40)$$

and define for the pulse λ an extended interaction subspace $\mathcal{I}_S \oplus \mathcal{I}_{P_{\lambda}}$ which includes both decoherence and pulse errors. By linearity of (38), $F_{(P_{\lambda}, \tau_{P_{\lambda}})}[\mathcal{I}_S \oplus \mathcal{I}_{P_{\lambda}}]$ is also a subspace. Consequently, first-order decoupling is still achieved if, for all generators P_{λ} , we have

$$F_{(P_{\lambda}, \tau_{P_{\lambda}})}[\mathcal{I}_S \oplus \mathcal{I}_{P_{\lambda}}] \subseteq \mathcal{C}_G. \quad (41)$$

Let us now consider the specific case of the Platonic sequences which are, by construction, Eulerian, and where the generators are simply global rotations. A decoupling Platonic sequence must be chosen according to Proposition 2 so that

$$\mathcal{I}_S \subseteq \bigotimes_{k=1}^N \bigoplus_{L=0}^{L_{\text{max}}^k} \mathcal{B}_{j_k}^{(L)} \subseteq \mathcal{C}_G. \quad (42)$$

First of all, as global rotations do not couple different irreps, it follows that

$$\mathcal{I}_S \oplus \mathcal{I}_{P_{\lambda}} \subseteq \mathcal{C}_G \Rightarrow F_{(P_{\lambda}, \tau_{P_{\lambda}})}(\mathcal{I}_S \oplus \mathcal{I}_{P_{\lambda}}) \subseteq \mathcal{C}_G \quad \forall \lambda. \quad (43)$$

Therefore, Platonic sequences are intrinsically robust to finite pulse duration errors.

It is also clear that Platonic sequences are robust to systematic errors satisfying $\mathcal{I}_{P_{\lambda}} \subseteq \bigotimes_{k=1}^N \bigoplus_{L=0}^{L_{\text{max}}^k} \mathcal{B}_{j_k}^{(L)} \subseteq \mathcal{C}_G \quad \forall \lambda$. In particular, they are all robust to *flip-angle errors*, defined as over- or under-rotation, and *axis specification errors*, where a target rotation about an axis \mathbf{n} is misimplemented about an axis $\mathbf{n}' = \sqrt{1-\epsilon} \mathbf{n} + \sqrt{\epsilon} \mathbf{n}_{\perp}$ [43], because both types of errors are linear with respect to the spin operators and thus belong to the $L = 1$ -irrep, which is in the correctable subspace of the three Platonic groups. This observation makes the sequences robust to control-induced disorder, where the amplitude of the control field implementing the pulses is not perfectly homogeneous across the spin ensemble, leading to all spins being rotated at slightly different rates. Each Platonic sequence is also robust to systematic pulse errors which are quadratic with respect to the spin operators, as the $L = 2$ -irrep also belongs to the correctable subspace of each group (except the D_2 group). Moreover, if the Platonic sequence is the universal decoupling strategy for a quantum system, then robustness to arbitrary and systematic pulse errors is guaranteed.

8 Dynamically corrected gates

While dynamical decoupling is commonly used to extend the lifetime of an idle qudit, a prescription for designing pulse sequences which mitigate decoherence while performing a non-trivial operation was introduced in Ref. [35]. In this section, we discuss the potential application of the framework presented in Secs. 5 and 6 for the design of such pulse sequences.

8.1 General theory

Consider a spin ensemble that interacts with an environment through an interaction Hamiltonian $H_{SB} = \sum_{\alpha} S_{\alpha} \otimes B_{\alpha}$ such that the interaction subspace satisfies

$$\mathcal{I}_S \subseteq \bigotimes_{k=1}^N \bigoplus_{L=0}^{L_{\text{max}}^k} \mathcal{B}_{j_k}^{(L)}, \quad (44)$$

and suppose we want to implement a control protocol described by the propagator

$$U_S(t) = \mathcal{T} \exp \left\{ -i \int_0^t H_u(t') dt' \right\}, \quad U_S(\tau_u) \equiv U_S, \quad (45)$$

which implements the unitary U_S in a finite time τ_u on the system of interest. During the implementation of the protocol, decoherence occurs and the actual propagator deviates slightly from the ideal unitary due to finite duration errors. This deviation can again be quantified through an EPO Φ_u , as defined in Eq. (36), which is well approximated (if decoherence is small enough) by [35]

$$\Phi_u \approx \Phi_u^{[1]} \equiv \sum_{\alpha} F_{(U, \tau_u)} [S_{\alpha}] \otimes B_{\alpha} \quad (46)$$

with the operation $F_{(U, \tau_u)}[\cdot]$ as defined in Eq. (38).

To reduce this deviation, we can use the formalism presented in Refs. [35, 37, 44] and construct a so-called *dynamically corrected gate* (DCG). To this end, we first need to construct a *balanced pair* $(\mathbb{1}_U(t), U^*(t))$, defined as a pair of pulses acting on the system and satisfying the three conditions below,

- (i) $\sum_{\alpha} F_{(\mathbb{1}_U, \tau_{\mathbb{1}})} [S_{\alpha}] \otimes B_{\alpha} = \sum_{\alpha} F_{(U^*, \tau_{U^*})} [S_{\alpha}] \otimes B_{\alpha}$,
- (ii) $\mathbb{1}_U(\tau_{\mathbb{1}}) = \mathbb{1}_S$,
- (iii) $U^*(\tau_{U^*}) = U_S$.

(47)

In other words, we need to find two pulses with identical EPOs, such that one implements the identity while the other implements the target unitary U_S . Once such a pair is constructed¹⁵, a DCG can be designed using the following four-step procedure:

¹⁵A simple prescription to construct a balanced pair is presented in Refs. [37, 44].

1. Pick a decoupling group \mathcal{G} and draw its Cayley graph
2. On each vertex, add the identity edge $\mathbb{1}_U$
3. Find an Eulerian path ending in an identity edge
4. Swap this last edge with the corresponding U^*

The resulting sequence then implements the target unitary U_S while the first-order EPO of the DCG reads

$$\Phi_{\text{DCG}}^{[1]} = \Phi_{\text{EDD}}^{[1]} + \sum_{\alpha} \Pi_{\mathcal{G}}(F_{(U^*, \tau_{u^*})}[S_{\alpha}]) \otimes B_{\alpha} \quad (48)$$

where $\Phi_{\text{EDD}}^{[1]}$ is simply the first-order error phase of the usual Eulerian path, as defined in Eq. (39), and satisfies $\Phi_{\text{EDD}}^{[1]} \propto \mathbb{1}_S \otimes B$ if the interaction subspace belongs to the correctable subspace of \mathcal{G} , *i.e.*, $\mathcal{I}_S \subseteq \mathcal{C}_{\mathcal{G}}$. The remaining condition for the DCG to provide first-order decoupling is then

$$F_{(U^*, \tau_{u^*})}[\mathcal{I}_S] \subseteq \mathcal{C}_{\mathcal{G}}. \quad (49)$$

When the propagator $U^*(t)$ is solely composed of rotations (global or local), we have that

$$\mathcal{I}_S \subseteq \bigotimes_{k=1}^N \bigoplus_{L=0}^{L_{\max}^k} \mathcal{B}_{j_k}^{(L)} \Rightarrow F_{(U^*, \tau_{u^*})}[\mathcal{I}_S] \subseteq \bigotimes_{k=1}^N \bigoplus_{L=0}^{L_{\max}^k} \mathcal{B}_{j_k}^{(L)}. \quad (50)$$

Consequently, the same Platonic sequence that was used to mitigate decoherence can also be used to construct a DCG. However, when $U^*(t)$ is not a rotation at all times, this is no longer true as $F_{(U^*, \tau_{u^*})}[\cdot]$ may couple different irreps. In this case, a universal decoupling group, if it exists, must be used to construct the DCG. The results mentioned above can be formulated as follows:

Proposition 3. *Consider an ensemble of N spins j_k interacting with its environment such that the interaction subspace*

$$\mathcal{I}_S \subseteq \bigotimes_{k=1}^N \bigoplus_{L=0}^{L_{\max}^k} \mathcal{B}_{j_k}^{(L)} \quad (51)$$

contains no 0-irreps (isotropic components) except the global identity. Then, any group not contained as a subgroup of $\mathcal{F}_{\max}(\mathcal{B}(\mathcal{H}^{(j_{\text{eff}})}))$, where $j_{\text{eff}} = \sum_{k=1}^N j_k$, can be used to construct any DCG. If the intended gate consists solely of local and global rotations and \mathcal{I}_S contains at most K -body terms, then j_{eff} must be replaced by half the sum of the K largest L_{\max}^k 's.

We should point out, however, that when the intended gate is not a global rotation, the subspace $F_{(U^*, \tau_{u^*})}[\mathcal{I}_S]$ may overlap with rotation-invariant subspaces even though \mathcal{I}_S does not. When constructing a DCG for a multispin system, we should then ensure that the balanced pair is designed in such a way this does not happen.

8.2 Applications

For a single spin- j system with an interaction subspace $\mathcal{I}_S \subseteq \bigoplus_{L=1}^{L_{\max}} \mathcal{B}^{(L)}$, we refer again to Table 4 to choose the appropriate decoupling group. In particular, we find that no Platonic group can be used to construct a DCG for an arbitrary quantum gate for $j \geq 3$ because there is no universal decoupling group consisting only of rotations in this case. This limits the use of Platonic DCG to protect operations outside of $\text{SU}(2)$ in high-dimensional qudits [40, 41, 45].

In the case of a set of identical spin- j with up to N -body terms, we now refer to Table 6a to choose the decoupling group. In particular, we find that no Platonic group can be used to construct a DCG for an arbitrary gate if $j \geq 3/2$. Nevertheless, for a qubit ensemble, the T group is sufficient to construct any DCG if the interaction subspace includes at most two-body interactions. A DCG can therefore be constructed to perform an entangling gate robust to finite-duration errors in a qubit ensemble. As mentioned above, one should however make sure that the balanced pair's EPO still respects the relevant anisotropy conditions. For example, for a pair of interacting qubits with an interaction Hamiltonian $H_S \in \mathcal{B}(\mathcal{H}^{(1/2)}) \otimes \mathcal{B}(\mathcal{H}^{(1/2)})$ and on which we wish to perform an entangling gate, the propagator $U^*(t)$ must satisfy the following condition

$$\begin{aligned} & \text{Tr} \left[\int_0^{\tau^*} (U^*(t))^{\dagger} H_S U^*(t) \mathbf{J}^1 \cdot \mathbf{J}^2 dt \right] = \\ \Leftrightarrow & \text{Tr} \left[H_S \int_0^{\tau^*} U^*(t) \mathbf{J}^1 \cdot \mathbf{J}^2 (U^*(t))^{\dagger} dt \right] = 0. \quad (52) \end{aligned}$$

A sufficient condition, provided that H_S itself satisfies the anisotropy conditions, is that $U^*(t)$ commutes with $\mathbf{J}^1 \cdot \mathbf{J}^2$ at all times. This is the case, for example, for a propagator of the form $U^*(t) = \exp\{-i\chi(t)J_{\mu}^1 \otimes J_{\mu}^2\}$ for any axis μ .

Finally, for a pair of spins with different quantum numbers $\{j_1, j_2\}$, we refer to Table 6b. In particular, the point group O can be used to construct an arbitrary DCG for a qubit-qutrit pair. For example, one could use this formalism to perform an entangling gate protected from finite-duration errors that transfers quantum information between the electron qubit and the nitrogen nucleus qutrit in an NV center, where the nuclear spin can be used as a quantum memory and the electronic spin for quantum computation [46, 47].

9 Conclusion

In this work, we have presented and studied three novel dynamical decoupling sequences (TEDD, OEDD and IEDD), called Platonic sequences, which are inspired by the three exceptional point groups describing the symmetries of the tetrahedron, octahedron and icosahedron. The information required for their construction can be found in Table 5. They exhibit remarkable decoupling properties for single- and multiqubit systems, and can be generated from just two specific global $SU(2)$ rotations, so there is no need for individual subsystem control. For single-qubit systems, Proposition 1 and Table 4 summarize our results, highlighting decoupling groups that cancel out different types of system-bath interaction that can perturb the system. A key result is the identification of at least one Platonic DD sequence that is universal for individual qudits with a number of levels $d < 7$, or equivalently, for individual spin- j with spin quantum number $j < 3$. Although Platonic sequences are longer than other known sequences, such as those presented in Ref. [16], they have the advantage that they can be implemented using only $SU(2)$ operations. Similarly, we showed that the Platonic sequences also decouple several types of interaction in multiqubit systems when the Hamiltonian does not contain isotropic components (see Table 6). We emphasize that the decoupling properties of each Platonic sequence depend only on the K -body terms and the irreps appearing in the interaction subspace of the subsystems. They are therefore independent of the number of qudits in the ensemble, unlike the sequences constructed in Refs. [8, 17, 20] (resp. Ref. [18]) whose lengths grow linearly (resp. quadratically) with the number of subsystems. For example, they can decouple up to five-body interactions in ensembles of qubits when the interaction Hamiltonian lacks isotropic components.

Platonic sequences are distinguished not only by their decoupling capabilities but also by their structural simplicity and elegance, stemming from their construction as Eulerian cycles on Cayley graphs of exceptional point groups (see Fig. 8). This construction underpins their inherent robustness to systematic pulse errors, finite duration effects, and other perturbations, which further enhances their practical applicability, making them highly relevant to a wide range of quantum systems. Furthermore, their decoupling and robustness properties could enable them to compete with longer sequences constructed numerically [10, 11, 22] and shorter sequences such as the well-known WAHUA [48] and REV-8 [49] cycles.

The simplest Platonic sequence, the TEDD sequence, has remarkable decoupling properties and requires a reasonable number of pulses to be implemented, which could make it a versatile tool in quantum information processing. It can decouple linear

and quadratic interactions in spin operators, leading to potential application in quantum computation using large spins [40, 41] and qudits [45]. It is also a universal decoupling sequence for a single qutrit, which naturally appears in NV centers [46, 47, 50]. In addition, it decouples any bilinear two-body interaction that is not isotropic, such as the dipole-dipole interaction and anisotropic spin exchange, among others [10, 22, 51], leading to a potential application in NMR spectroscopy [14, 48, 49].

To arrive at our findings, we had to generalize the Majorana representation of Hermitian operators to non-Hermitian operators, which allowed us to study the possible point groups of bounded operators acting on a finite-dimensional Hilbert space. This may be useful beyond the main focus of this work, for example in the study of quantum correlations, where extremal quantum states [52, 53] and extremal quantum gates [54] for spin systems have a high degree of rotational symmetry.

Overall, the results presented in this study contribute to the expansion of the frontiers of dynamical decoupling and Hamiltonian engineering by providing novel sequences with both theoretical and practical advantages. Platonic sequences offer a promising avenue for future research and applications, e.g., in quantum computing, particularly in environments where robustness to errors is crucial. Their appeal also lies in the fact that they are compatible with more advanced dynamical decoupling strategies, such as dynamically corrected gates, as discussed in Sec. 8, but also concatenated dynamical decoupling [55, 56].

Acknowledgments

ESE acknowledges support from the postdoctoral fellowship of the IPD-STEMA program of the University of Liège (Belgium). JM acknowledges the FWO and the F.R.S.-FNRS for their funding as part of the Excellence of Science program (EOS project 40007526). CR is a Research Fellow of the F.R.S.-FNRS. Computational resources were provided by the Consortium des Equipements de Calcul Intensif (CECI), funded by the Fonds de la Recherche Scientifique de Belgique (F.R.S.-FNRS) under Grant No. 2.5020.11. The figures in this manuscript were produced using the Makie package [57] of the Julia programming language.

References

- [1] John Preskill. “Quantum Computing in the NISQ era and beyond”. *Quantum* **2**, 79 (2018).
- [2] Kishor Bharti, Alba Cervera-Lierta, Thi Ha Kyaw, Tobias Haug, Sumner Alperin-Lea, Abhinav Anand, Matthias Degroote, Hermanni Heimonen, Jakob S. Kottmann, Tim Menke, Wai-

- Keong Mok, Sukin Sim, Leong-Chuan Kwek, and Alán Aspuru-Guzik. “Noisy intermediate-scale quantum algorithms”. *Rev. Mod. Phys.* **94**, 015004 (2022).
- [3] Lorenza Viola, Emanuel Knill, and Seth Lloyd. “Dynamical decoupling of open quantum systems”. *Phys. Rev. Lett.* **82**, 2417 (1999).
- [4] Lorenza Viola and Emanuel Knill. “Robust dynamical decoupling of quantum systems with bounded controls”. *Phys. Rev. Lett.* **90**, 037901 (2003).
- [5] Götz S. Uhrig. “Keeping a quantum bit alive by optimized π -pulse sequences”. *Phys. Rev. Lett.* **98**, 100504 (2007).
- [6] Michael J. Biercuk, Hermann Uys, Aaron P. Vandevender, Nobuyasu Shiga, Wayne M. Itano, and John J. Bollinger. “Optimized dynamical decoupling in a model quantum memory”. *Nature* **458**, 996 (2009).
- [7] Gregory Quiroz and Daniel A. Lidar. “Optimized dynamical decoupling via genetic algorithms”. *Phys. Rev. A* **88**, 052306 (2013).
- [8] Marcus Stollsteimer and Günter Mahler. “Suppression of arbitrary internal coupling in a quantum register”. *Phys. Rev. A* **64**, 052301 (2001).
- [9] Gerardo A Paz-Silva, Seung-Woo Lee, Todd J Green, and Lorenza Viola. “Dynamical decoupling sequences for multi-qubit dephasing suppression and long-time quantum memory”. *New Journal of Physics* **18**, 073020 (2016).
- [10] Joonhee Choi, Hengyun Zhou, Helena S. Knowles, Renate Landig, Soonwon Choi, and Mikhail D. Lukin. “Robust dynamic hamiltonian engineering of many-body spin systems”. *Phys. Rev. X* **10**, 031002 (2020).
- [11] Pai Peng, Xiaoyang Huang, Chao Yin, Linta Joseph, Chandrasekhar Ramanathan, and Paola Cappellaro. “Deep reinforcement learning for quantum hamiltonian engineering”. *Phys. Rev. Appl.* **18**, 024033 (2022).
- [12] C. E. Bradley, J. Randall, M. H. Abobeih, R. C. Berrevoets, M. J. Degen, M. A. Bakker, M. Markham, D. J. Twitchen, and T. H. Taminiiau. “A ten-qubit solid-state spin register with quantum memory up to one minute”. *Phys. Rev. X* **9**, 031045 (2019).
- [13] Jonas Bylander, Simon Gustavsson, Fei Yan, Fumiki Yoshihara, Khalil Harrabi, George Fitch, David G. Cory, Yasunobu Nakamura, Jaw-Shen Tsai, and William D. Oliver. “Noise spectroscopy through dynamical decoupling with a superconducting flux qubit”. *Nature Physics* **7**, 565 (2011).
- [14] Rangeet Bhattacharyya, Ipsita Chakraborty, Arnab Chakrabarti, and Swagata Mandal. “Chapter two - recent studies on accurate measurements of nmr transverse relaxation times”. In Graham A. Webb, editor, *Annual Reports on NMR Spectroscopy. Volume 99 of Annual Reports on NMR Spectroscopy*, pages 57–77. Academic Press (2020).
- [15] R.M. Goldblatt, A.M. Martin, and A.A. Wood. “Sensing coherent nuclear spin dynamics with an ensemble of paramagnetic nitrogen spins”. *PRX Quantum* **5**, 020334 (2024).
- [16] Vinay Tripathi, Noah Goss, Arian Vezvaei, Long B. Nguyen, Irfan Siddiqi, and Daniel A. Lidar. “Qudit dynamical decoupling on a superconducting quantum processor” (2024). [arXiv:2407.04893](https://arxiv.org/abs/2407.04893).
- [17] Pawel Wocjan, Martin Rötteler, Dominik Janzing, and Thomas Beth. “Simulating hamiltonians in quantum networks: Efficient schemes and complexity bounds”. *Phys. Rev. A* **65**, 042309 (2002).
- [18] Pawel Wocjan. “Efficient decoupling schemes with bounded controls based on eulerian orthogonal arrays”. *Phys. Rev. A* **73**, 062317 (2006).
- [19] M. Rotteler and P. Wocjan. “Equivalence of decoupling schemes and orthogonal arrays”. *IEEE Transactions on Information Theory* **52**, 4171 (2006).
- [20] Martin Rötteler and Pawel Wocjan. “Combinatorial approaches to dynamical decoupling”. *Page 376–394*. Cambridge University Press. (2013).
- [21] Soonwon Choi, Norman Y. Yao, and Mikhail D. Lukin. “Dynamical engineering of interactions in qudit ensembles”. *Phys. Rev. Lett.* **119**, 183603 (2017).
- [22] Hengyun Zhou, Haoyang Gao, Nathaniel T. Leitao, Oksana Makarova, Iris Cong, Alexander M. Douglas, Leigh S. Martin, and Mikhail D. Lukin. “Robust hamiltonian engineering for interacting qudit systems”. *Phys. Rev. X* **14** (2024).
- [23] Béla Bollobás. “Graphs, groups and matrices”. *Pages 253–293*. Springer New York. New York, NY (1998).
- [24] E. Majorana. “Atomi orientati in campo magnetico variabile”. *Nuovo Cimento* **9**, 43 (1932).
- [25] E. Serrano-Ensástiga and D. Braun. “Majorana representation for mixed states”. *Phys. Rev. A* **101**, 022332 (2020).
- [26] L. M. K. Vandersypen and I. L. Chuang. “Nmr techniques for quantum control and computation”. *Rev. Mod. Phys.* **76**, 1037–1069 (2005).

- [27] S. Damodarakurup, M. Lucamarini, G. Di Giuseppe, D. Vitali, and P. Tombesi. “Experimental inhibition of decoherence on flying qubits via “bang-bang” control”. *Phys. Rev. Lett.* **103**, 040502 (2009).
- [28] Hugo Ferretti, Y. Batuhan Yilmaz, Kent Bonsma-Fisher, Aaron Z. Goldberg, Noah Lupu-Gladstein, Arthur O. T. Pang, Lee A. Rozema, and Aephraim M. Steinberg. “Generating a 4-photon tetrahedron state: toward simultaneous super-sensitivity to non-commuting rotations”. *Optica Quantum* **2**, 91–102 (2024).
- [29] David C. Spierings, Joseph H. Thywissen, and Aephraim M. Steinberg. “Spin rotations in a bose-einstein condensate driven by counterflow and spin-independent interactions”. *Phys. Rev. Lett.* **132**, 173401 (2024).
- [30] Mildred S Dresselhaus, Gene Dresselhaus, and Ado Jorio. “Group theory: application to the physics of condensed matter”. *Springer Science & Business Media*. (2007).
- [31] C. J. Bradley and A. P. Cracknell. “The mathematical theory of symmetry in solids: Representation theory for point groups and space groups”. *Oxford University Press*. (2009).
- [32] U. Fano. “Geometrical characterization of nuclear states and the theory of angular correlations”. *Phys. Rev.* **90**, 577 (1953).
- [33] D A Varshalovich, A N Moskalev, and V K Khersonskii. “Quantum theory of angular momentum”. *World Scientific*. (1988).
- [34] A. V. Shubnikov and N. V. Belov. “Colored symmetry”. Pergamon Press, Oxford. (1964).
- [35] Kaveh Khodjasteh and Lorenza Viola. “Dynamically error-corrected gates for universal quantum computation”. *Phys. Rev. Lett.* **102** (2009).
- [36] Paolo Zanardi. “Symmetrizing evolutions”. *Physics Lett. A* **258**, 77 (1999).
- [37] Kaveh Khodjasteh and Lorenza Viola. “Dynamical quantum error correction of unitary operations with bounded controls”. *Phys. Rev. A* **80** (2009).
- [38] Lorenza Viola. “Introduction to quantum dynamical decoupling”. Page 105–125. Cambridge University Press. (2013).
- [39] Matthew D Grace, Jason Dominy, Robert L Kosut, Constantin Brif, and Herschel Rabitz. “Environment-invariant measure of distance between evolutions of an open quantum system”. *New Journal of Physics* **12**, 015001 (2010).
- [40] Sivaprasad Omanakuttan. “Quantum computation using large spin qudits” (2024). [arXiv:2405.07885](https://arxiv.org/abs/2405.07885).
- [41] Sivaprasad Omanakuttan, Vikas Buchemavari, Jonathan A. Gross, Ivan H. Deutsch, and Milad Marvian. “Fault-tolerant quantum computation using large spin-cat codes”. *PRX Quantum* **5**, 020355 (2024).
- [42] Marcis Auzinsh, Dmitry Budker, and Simon Rochester. “Optically polarized atoms: Understanding light–atom interactions”. Oxford University Press. (2010).
- [43] Nic Ezzell, Bibek Pokharel, Lina Tewala, Gregory Quiroz, and Daniel A. Lidar. “Dynamical decoupling for superconducting qubits: A performance survey”. *Phys. Rev. Appl.* **20**, 064027 (2023).
- [44] Kaveh Khodjasteh, Daniel A. Lidar, and Lorenza Viola. “Arbitrarily accurate dynamical control in open quantum systems”. *Phys. Rev. Lett.* **104**, 090501 (2010).
- [45] Martin Ringbauer, Michael Meth, Lukas Postler, Roman Stricker, Rainer Blatt, Philipp Schindler, and Thomas Monz. “A universal qudit quantum processor with trapped ions”. *Nature Physics* **18**, 1053 (2022).
- [46] Sen Yang, Ya Wang, D. D. Bhaktavatsala Rao, Thai Hien Tran, Ali S. Momenzadeh, M. Markham, D. J. Twitchen, Ping Wang, Wen Yang, Rainer Stöhr, Philipp Neumann, Hideo Kosaka, and Jörg Wrachtrup. “High-fidelity transfer and storage of photon states in a single nuclear spin”. *Nature Photonics* **10**, 507 (2016).
- [47] N. Kalb, P. C. Humphreys, J. J. Slim, and R. Hanson. “Dephasing mechanisms of diamond-based nuclear-spin memories for quantum networks”. *Phys. Rev. A* **97**, 062330 (2018).
- [48] J. S. Waugh, L. M. Huber, and U. Haeberlen. “Approach to high-resolution nmr in solids”. *Phys. Rev. Lett.* **20**, 180 (1968).
- [49] W-K. Rhim, D. D. Elleman, and R. W. Vaughan. “Enhanced resolution for solid state NMR”. *The Journal of Chemical Physics* **58**, 1772 (1973).
- [50] Yue Fu, Wenquan Liu, Xiangyu Ye, Ya Wang, Chengjie Zhang, Chang-Kui Duan, Xing Rong, and Jiangfeng Du. “Experimental investigation of quantum correlations in a two-qutrit spin system”. *Phys. Rev. Lett.* **129**, 100501 (2022).
- [51] Dmitry Zakharov, Hans-Albrecht Krug von Nidda, Mikhail Eremin, Joachim Deisenhofer, Rushana Eremina, and Alois Loidl. “Anisotropic exchange in spin chains”. In Bernard Barbara, Yosef Imry, G. Sawatzky, and P. C. E. Stamp, editors, *Quantum Magnetism*. Pages 193–238. Dordrecht (2008). Springer Netherlands.
- [52] J. Martin, O. Giraud, P. A. Braun, D. Braun, and T. Bastin. “Multiqubit symmetric states with

high geometric entanglement”. *Phys. Rev. A* **81**, 062347 (2010).

- [53] C. Chryssomalakos, L. Hanotel, E. Guzmán-González, D. Braun, E. Serrano-Ensástiga, and K. Życzkowski. “Symmetric multiqubit states: Stars, entanglement, and rotoensors”. *Phys. Rev. A* **104**, 012407 (2021).
- [54] D. Morachis Galindo and Jesús A. Maytorena. “Entangling power of symmetric two-qubit quantum gates and three-level operations”. *Phys. Rev. A* **105**, 012601 (2022).
- [55] K. Khodjasteh and D. A. Lidar. “Fault-tolerant quantum dynamical decoupling”. *Phys. Rev. Lett.* **95**, 180501 (2005).
- [56] Colin Read, Eduardo Serrano-Ensástiga, and John Martin. Work in progress.
- [57] Danisch & Krumbiegel. “Makie.jl: Flexible high-performance data visualization for julia”. *Journal of Open Source Software* **6**, 3349 (2021).
- [58] Joseph J Rotman. “An introduction to the theory of groups”. Volume 148. Springer Science & Business Media. (2012).
- [59] Harold Scott Macdonald Coxeter. “Regular polytopes”. Dover, New York. (1973). 3rd edition.
- [60] Igor Pak and Radoš Radoičić. “Hamiltonian paths in cayley graphs”. *Discrete Mathematics* **309**, 5501 (2009).
- [61] Carl Hierholzer. “Ueber die möglichkeit, einen linienzug ohne wiederholung und ohne unterbrechung zu umfahren”. *Mathematische Annalen* **6**, 30 (1873). url: <http://eudml.org/doc/156599>.
- [62] C. Chryssomalakos, E. Guzmán-González, and E. Serrano-Ensástiga. “Geometry of spin coherent states”. *J. Phys. A: Math. Theor.* **51**, 165202 (2018).
- [63] P. G. Appleby, B. R. Duffy, and R. W. Ogden. “On the classification of isotropic tensors”. *Glasgow Mathematical Journal* **29**, 185 (1987).
- [64] Harold Jeffreys. “On isotropic tensors”. *Mathematical Proceedings of the Cambridge Philosophical Society* **73**, 173–176 (1973).
- [65] Philip G. Hodge. “On isotropic cartesian tensors”. *The American Mathematical Monthly* **68**, 793 (1961).
- [66] Elliot A. Kearsley and Jeffrey T. Fong. “Linearly independent sets of isotropic cartesian tensors of ranks up to eight”. *Journal of Research of the National Bureau of Standards, Section B: Mathematical Sciences* **79B**, 49 (1975).

A Exceptional point groups and their generators

Let us consider a group \mathcal{G} and a subset of elements $\Gamma = \{a, b, \dots\} \subseteq \mathcal{G}$. Γ is called a *generating set*, and its elements are called *generators*, if each element of \mathcal{G} can be uniquely expressed as a product of elements of Γ . Furthermore, the group generated by Γ admits a *presentation* in terms of its generators and a set of *defining relations* [23, 58]. A defining relation is a sequence of generators that implements the identity. For example, we write $\mathcal{G} = \langle a, b | a^2, b^2, ab \rangle$ the group generated by the generators $\{a, b\}$ satisfying $a^2 = b^2 = ab = E$ where E is the identity element. Each proper exceptional group associated with the Platonic solids has two generators, and a presentation of these is given by [58]

$$\begin{aligned} \text{T} &= \langle a, b | a^3, b^3, (ab)^2 \rangle, \\ \text{O} &= \langle a, b | a^4, b^3, (ab)^2 \rangle, \\ \text{I} &= \langle a, b | a^5, b^3, (ab)^2 \rangle. \end{aligned} \quad (53)$$

Other presentations of the groups are $\langle a, b | a^2, b^3, (ab)^k \rangle$ where $k = 3, 4, 5$ for T, O and I, respectively [58].

A.1 Tetrahedral group T

The tetrahedral point group consists of 12 transformations $\text{T} = \{E, 8C_3, 3C_2\}$ where we use the notation defined in Section 2. The C_3 rotations are performed around an axis passing through the vertices (or the barycentre of the faces) of the tetrahedron, and the C_2 rotations are performed around axes passing through the midpoints of two complementary edges (those without common vertices). We write below the twelve explicit rotations sorted in each class in terms of the axis-angle notation (\mathbf{n}, θ) . Setting

$$\begin{aligned} \mathbf{n}_0 &= (0, 0, 1), & \mathbf{n}_1^\pm &= \left(\frac{\sqrt{2}}{3}, \pm \sqrt{\frac{2}{3}}, \frac{1}{3} \right), \\ \mathbf{n}_2 &= \left(\frac{2\sqrt{2}}{3}, 0, -\frac{1}{3} \right), & \mathbf{n}_3 &= \left(\sqrt{\frac{2}{3}}, 0, \frac{1}{\sqrt{3}} \right), \\ \mathbf{n}_4^\pm &= \left(-\frac{1}{\sqrt{6}}, \pm \frac{1}{\sqrt{2}}, \frac{1}{\sqrt{3}} \right), \end{aligned}$$

we have

$$\begin{aligned} E &= (\mathbf{n}_0, 0), \\ 8C_3 &= \left\{ \left(\pm \mathbf{n}_0, \frac{2\pi}{3} \right), \left(\pm \mathbf{n}_1^\pm, \frac{2\pi}{3} \right), \left(\pm \mathbf{n}_2, \frac{2\pi}{3} \right) \right\}, \\ 3C_2 &= \left\{ (\mathbf{n}_3, \pi), (\mathbf{n}_4^\pm, \pi) \right\}. \end{aligned}$$

The presentation (53) of T can be obtained with the generators

$$a = \left(\mathbf{n}_0, \frac{2\pi}{3} \right), \quad b = \left(\mathbf{n}_1^+, \frac{2\pi}{3} \right). \quad (54)$$

The whole group is thus given by E and

$$\begin{aligned} 8C_3 &= \{a, a^2\} \bigcup_{\substack{k=1,2 \\ j=0,1,2}} \{a^{-j}b^k a^j\} \\ 3C_2 &= \{a^{-j}ba^{j+1}\}_{j=0,1,2} \end{aligned} \quad (55)$$

A.2 Octahedral group O

The octahedral point group (equivalent to the point group of a cube) has 24 elements. It is made up as follows $O = \{E, 8C_3, 6C_2, 6C_4, 3C_2(=C_4^2)\}$. The octahedron can be oriented such that its vertices are in the Cartesian axes

$$(\pm 1, 0, 0), \quad (0, \pm 1, 0), \quad (0, 0, \pm 1). \quad (56)$$

The generators of its point group can be taken as

$$a = \left(\mathbf{n}_0, \frac{\pi}{2}\right), \quad b = \left(\frac{1}{\sqrt{3}}(1, 1, 1), \frac{2\pi}{3}\right). \quad (57)$$

The rotations $6C_4$ and $3C_2$ are the $2\pi n/4$ rotations about the axes of symmetry passing through the vertices of the octahedron. They are spanned by the operations

$$\{b^{-j}a^{k+1}b^j\}_{j,k=0,1,2}. \quad (58)$$

The $8C_3$ rotations are the $2\pi n/3$ rotations about an axis passing through the faces of the octahedron, generated by

$$\{a^{-j}b^k a^j\}_{\substack{k=1,2 \\ j=0,1,2,3}}. \quad (59)$$

Finally, the $6C_2$ ($2\pi/2 = \pi$) rotations are about an axis passing through the edges of the octahedron, and can be generated by

$$\{b^{-j}a^{k+1}ba^{-k}b^j\}_{\substack{j=0,1,2 \\ k=0,1}}. \quad (60)$$

A.3 Icosahedral group I

The last exceptional proper point group is $I = \{E, 12C_5, 12C_5^2, 20C_3, 15C_2\}$ with 60 elements and associated to the proper symmetries of the icosahedron or the dodecahedron. A possible orientation of the icosahedron corresponds to the following 12 non-normalised vertices [59]

$$(\pm 1, \pm \phi, 0), \quad (0, \pm 1, \pm \phi), \quad (\pm \phi, 0, \pm 1), \quad (61)$$

where $\phi = \frac{\sqrt{5}+1}{2}$ is the golden ratio. One type of generators for the presentation (53) of I is given by

$$a = \left(\frac{(0, -1, \phi)}{\sqrt{\phi+2}}, \frac{2\pi}{5}\right), \quad b = \left(\frac{(1-\phi, 0, \phi)}{\sqrt{3}}, \frac{2\pi}{3}\right). \quad (62)$$

The rotations $12C_5$ and $12C_5^2$ are the symmetries associated to $2\pi n/5$ rotations about an axis passing through the vertices of the icosahedron with elements

$$\{a^k\}_{k=1}^4 \bigcup_{\substack{j=1,2,3,4 \\ k=0,1,2,3,4}} \{a^k b a^j b^{-1} a^{-k}\}. \quad (63)$$

The $20C_3$ rotations are the rotations about an axis passing through the barycentre of the faces, and they are generated by

$$\{a^j A^{-(l-1)} b^k A^{(l-1)} a^{-j}\}_{\substack{k,l=1,2 \\ j=0,1,2,3,4}} \quad (64)$$

with $A = bab^{-1}$. Lastly, the symmetries associated to rotations about an axis passing through the midpoint of the edges of the icosahedron are generated by

$$\{a^{k+1}ba^{-k}, a^k X a^{-k}, a^k Y a^{-k}\}_{k=0,1,2,3,4}, \quad (65)$$

with

$$X = b^{-1}ab^2, \quad Y = (a^{-1}ba)^{-1}X(a^{-1}ba). \quad (66)$$

B Cayley graphs and Eulerian cycles

We call the *Cayley graph* (or diagram) of \mathcal{G} with respect to Γ , $G(\mathcal{G}, \Gamma)$, the graph constructed by assigning a vertex to each element of \mathcal{G} and linking pairs of vertices by directed, colored edges, where each color represents a generator. An edge departing from x and heading to y has the color of the generator g iff $y = gx$. On such a graph, each vertex has $|\Gamma|$ ingoing and departing edges, where $|\Gamma|$ is the cardinality of Γ (the number of generators). This implies that there exists an Eulerian cycle¹⁶ on such graph [23]. Furthermore, in some cases a Hamiltonian cycle¹⁷ could also exist [60]. In the Cayley graph representation, the defining relations are identified by closed loops.

A simple prescription for constructing a Cayley graph of the group \mathcal{G} based on its generating set and defining relations is presented in Ref. [23]. The basic idea is to start with a single vertex and expand the graph by noting that at each vertex, two properties must be satisfied: (i) there must be exactly $|\Gamma|$ outgoing and incoming edges, one of each color, and (ii) every defining relation must be satisfied. So we add the vertices one by one, and each time a vertex is added, we add the edges by closing the loops corresponding to the different defining relations. The procedure is illustrated in Fig. 7 for $T = \langle a, b | a^3, b^3, (ab)^2 \rangle$. Each presentation (53) of the exceptional point groups has an elegant three-dimensional Cayley graph representation (see Fig. 8) with Eulerian cycles that can easily be found using Hierholzer's algorithm [61]); such cycles for the groups T , O and I are, for example, given by

$$\begin{aligned} \text{TEDD} &\equiv abaababbbbaababbbbaababbaa \\ &= aba^2bab^3a^2bab^3a^2bab^2b^2, \end{aligned} \quad (67)$$

¹⁶An Eulerian cycle is a closed loop that uses each edge of the graph exactly once.

¹⁷A Hamiltonian cycle is a closed loop that visits each node of the graph exactly once.

$$\begin{aligned}
\text{OEDD} &\equiv abaaabbbabaabbaababbaaa \\
&\quad ababbbabaabbaaababbbabb \\
&= aba^3b^3aba^2b^3a^2bab^2a^4bab^3 \\
&\quad aba^2b^2a^4bab^3ab^2,
\end{aligned} \tag{68}$$

$$\begin{aligned}
\text{IEDD} &\equiv baaabbaabaaaaabbaaab \\
&\quad abbbabaabbaabbbabb \\
&\quad abbbaaaababbbbaaababb \\
&\quad baaababbbbaabbaabba \\
&\quad abbaabbbabbbbaababba \\
&\quad ababbbbaabbbbaaaaa \\
&= ba^3b^2a^2ba^5b^2a^3bab^3aba^2 \\
&\quad b^2a^2b^2ab^2ab^2ab^3a^4bab^3a^3 \\
&\quad bab^3a^3bab^3a^2bab^2a^2b^2a^2 \\
&\quad b^2a^2b^3ab^3a^2bab^3a^2bab^3a^2 \\
&\quad bab^3aba^5.
\end{aligned} \tag{69}$$

where the generators for each group are summarized below (see also Table 5)

$$\text{T} \rightarrow \begin{cases} a = ((0, 0, 1), \frac{2\pi}{3}) \\ b = \left(\left(\frac{\sqrt{2}}{3}, \sqrt{\frac{2}{3}}, \frac{1}{3} \right), \frac{2\pi}{3} \right) \end{cases} \tag{70}$$

$$\text{O} \rightarrow \begin{cases} a = ((0, 0, 1), \frac{2\pi}{4}) \\ b = \left(\frac{1}{\sqrt{3}}(1, 1, 1), \frac{2\pi}{3} \right) \end{cases} \tag{71}$$

$$\text{I} \rightarrow \begin{cases} a = \left(\frac{1}{\sqrt{\phi+2}}(0, -1, \phi), \frac{2\pi}{5} \right) \\ b = \left(\frac{1}{\sqrt{3}}(1 - \phi, 0, \phi), \frac{2\pi}{3} \right) \end{cases} \tag{72}$$

with $\phi = \frac{\sqrt{5}+1}{2}$. We specify in Eqs. (67)–(69) the full sequence for each group as well as a (slightly) more compact and intelligible formulation. Note that there is no Hamiltonian cycle on the (directed) Cayley graph of any of the three exceptional point groups, so the Eulerian cycles are the smallest pulse sequences that implement the decoupling scheme.

C Majorana representation of pure spin states

The Majorana or *stellar* representation for pure spin- j states [24, 62] maps each element $|\psi\rangle \in \mathcal{H}^{(j)}$ of the Hilbert space $\mathcal{H}^{(j)}$ of dimension $2j + 1$ to $N = 2j$ points on the sphere S^2 . This representation contains all the information about the state after removing its normalization and the global phase factor. Majorana [24] introduced this representation via a polynomial constructed from the expansion of the state in the J_z eigenbasis, $|\psi\rangle = \sum_{m=-j}^j \lambda_m |j, m\rangle$ and given by

$$p_\psi(z) = \sum_{m=-j}^j (-1)^{j-m} \sqrt{\binom{2j}{j-m}} \lambda_m z^{j+m}. \tag{73}$$

The complex roots of the polynomial are complemented by as many roots at the infinity as are needed to be $2j$ in number. This set of roots $\{\zeta_k\}_{k=1}^{2j}$ is then mapped to a collection of points on the sphere via stereographic projection from the South Pole, poetically referred to as a *constellation* \mathfrak{C}_ψ of $|\psi\rangle$. Specifically, each root $\zeta = \tan(\theta/2)e^{i\phi}$ is projected onto a point (*star*) on the sphere with polar and azimuthal angles (θ, ϕ) .

In contrast to the Majorana representation for Hermitian operators, the point group of a pure state $|\psi\rangle$ can be obtained simply by analyzing this standard Majorana constellation where there is no distinction (coloring) among the stars. As an example, the Majorana representation of the spin-2 pure state

$$|\psi\rangle = \frac{1}{\sqrt{3}} \left(|2, 2\rangle + \sqrt{2} |2, -1\rangle \right). \tag{74}$$

has constellation equal to the tetrahedron. Consequently, the point group of $|\psi\rangle$ is equal to the tetrahedral group T.

D Correspondence between constellation colouring and a Hermitian operator

Following Ref. [25], we present here how to associate an equivalence class to a Hermitian operator $H = \mathbf{h}_L \cdot \mathbf{T}_L \in \mathcal{B}^{(L)}$ with constellation \mathfrak{C}_L . More precisely, we want to associate an equivalence class $[\mathfrak{C}_L]$ of colorings of \mathfrak{C}_L with the unit vector $\hat{h}_L = \mathbf{h}_L/h_L$. First, we denote by $\pm \mathbf{n}_k$ the stars of \mathfrak{C}_L . Each coloring \mathbf{c} of \mathfrak{C}_L can be now defined by an L -tuple of these points as follows

$$\mathbf{c} = \{\gamma_1 \mathbf{n}_1, \gamma_2 \mathbf{n}_2, \dots, \gamma_L \mathbf{n}_L\}, \tag{75}$$

with $\gamma_k = \pm 1$. The two equivalence classes, denoted by $[\mathfrak{C}_L^\pm]$, are now defined as¹⁸

$$[\mathfrak{C}_L^\pm] \equiv \left\{ \mathbf{c} \mid \prod_{k=1}^L \gamma_k = \pm 1 \right\}. \tag{76}$$

On the other hand, each tuple $\mathbf{c}^\pm \in [\mathfrak{C}_L^\pm]$ defines a unique spin- L pure state as [25]

$$h_{LM}^\pm = N_\phi \langle j, j, L, M | (|\phi\rangle \otimes A |\phi\rangle), \tag{77}$$

with $|\phi\rangle = \sum_m \lambda_m |j, m\rangle$ an $(L/2)$ -spinor with Majorana constellation defined by \mathbf{c}^\pm , $|\phi^A\rangle$ the corresponding antipodal state

$$|\phi^A\rangle \equiv \sum_m (-1)^{j+m} \lambda_{-m}^* |j, m\rangle, \tag{78}$$

N_ϕ a positive factor that guarantees the normalization of $\hat{h}_L^\pm = (h_{LL}^\pm, \dots, h_{L-L}^\pm)$, and $|j, j, L, M\rangle$ the common

¹⁸The choice of signs for $\pm \mathbf{n}_k$ is not uniquely defined and is associated with the labelling of the equivalence classes. This is analogous to a gauge freedom to specify the classes $[\mathfrak{C}_L]$. Once $\pm \mathbf{n}_k$ has been chosen, the classes $[\mathfrak{C}_L^\pm]$ are uniquely defined.

eigenvectors of the total angular momentum operators \mathbf{J}^2 and J_z where $J_a = J_a^1 + J_a^2$ with $a = x, y, z$. It turns out that \hat{h}_L^\pm depends only on the equivalence class of \mathfrak{c}^\pm [25]. Thus, we have uniquely specified \hat{h}_L^\pm to each equivalence class $[\mathfrak{C}_L^\pm]$, the two differing only by a sign $\hat{h}_L^+ = -\hat{h}_L^-$ [25]. With the vectors \hat{h}_L^\pm , we can now uniquely associate a class $[\mathfrak{C}_L^\pm]$ to any operator $H \in \mathcal{B}^{(L)}$ with uncolored constellation \mathfrak{C}_L . The corresponding class $[\mathfrak{C}_L]$ of an operator H , with associated vector \hat{h}_L , is $[\mathfrak{C}_L^+]$ (resp. $[\mathfrak{C}_L^-]$) if $\hat{h}_L = \hat{h}_L^+$ (resp. $\hat{h}_L = \hat{h}_L^-$).

E Rotation-invariant component of a Hamiltonian

As explained in the main text, applying global rotations on an ensemble of interacting subsystems will leave invariant a part of the Hamiltonian, which we call the rotation-invariant or isotropic component of the Hamiltonian. In order to identify this isotropic part, we first determine how the total Hamiltonian transforms under rotation and find the conditions for the Hamiltonian to be invariant under these transformations. This approach is similar to that of Ref. [21], where the authors identified $SU(d)$ -invariant components in the interaction Hamiltonian of a pair of qudits.

Here we describe how to obtain the rotation-invariant part of a generic Hamiltonian for the special cases of only multilinear interaction terms between the constituents of a N -spin system and for any two-body interactions.

E.1 Multilinear interactions between N spins

We consider an ensemble of N spins of quantum numbers $\{j_k\}_{k=1}^N$ with an interaction Hamiltonian H with fixed K -body terms multilinear in the spin operators. By simplicity, let us start by considering the case $K = N$. Since we are only interested in multilinear interactions, the Hamiltonian belongs to the following interaction subspace

$$H \in \mathcal{I}_S = \bigotimes_{k=1}^N \mathcal{I}_S^k \quad \text{with} \quad \mathcal{I}_S^k \subseteq \mathcal{B}_{j_k}^{(1)} \quad (79)$$

where $\mathcal{B}_{j_k}^{(1)} = \text{span}(\{J_{\alpha_k}\}_{\alpha_k=x,y,z})$, with J_{α_k} are the corresponding $(2j_k + 1) \times (2j_k + 1)$ matrices representing the angular momentum operators. The interaction Hamiltonian can be decomposed in the orthonormal operator basis $\left\{ \frac{1}{\sqrt{\Gamma}} \bigotimes_{k=1}^N J_{\alpha_k} \right\}$ where $\Gamma = \prod_{k=1}^N \frac{j_k(j_k+1)(2j_k+1)}{3}$ is a normalization factor¹⁹; we define the interaction tensor h as the rank- N tensor

¹⁹The basis is orthonormal with respect to the trace norm.

$h_{\alpha_1, \dots, \alpha_N}$ resulting from the following decomposition

$$H = \frac{1}{\sqrt{N}} \sum_{\alpha} h_{\alpha} \bigotimes_{k=1}^N J_{\alpha_k}, \quad (80)$$

or

$$h_{\alpha} = \frac{1}{\sqrt{\Gamma}} \text{Tr} \left[H \bigotimes_{k=1}^N J_{\alpha_k} \right], \quad (81)$$

where $\alpha = (\alpha_1, \dots, \alpha_N)$. Suppose that we apply an identical rotation \mathbf{R} on each subspace via its corresponding irrep through the Wigner-D matrices $D^{(j_k)}(\mathbf{R}) = D^{(j_k)}$, and set $G = \bigotimes_{k=1}^N D^{(j_k)}$. The interaction tensor transforms as follows

$$\begin{aligned} \tilde{h}_{\alpha} &= \frac{1}{\sqrt{\Gamma}} \text{Tr} \left[G^\dagger H G \bigotimes_{k=1}^N J_{\alpha_k} \right] \\ &= \frac{1}{\Gamma} \sum_{\beta} h_{\beta} \text{Tr} \left[\left(\bigotimes_{k=1}^N D^{(j_k)\dagger} J_{\beta_k} D^{(j_k)} \right) \bigotimes_{k=1}^N J_{\alpha_k} \right] \\ &= \frac{1}{\Gamma} \sum_{\beta} h_{\beta} \prod_{k=1}^N \text{Tr} \left[D^{(j_k)\dagger} J_{\beta_k} D^{(j_k)} J_{\alpha_k} \right]. \end{aligned} \quad (82)$$

Since a $SU(2)$ operation D acts on the spin operator \mathbf{J} with its corresponding physical three-dimensional rotation matrix $\mathbf{O}(\mathbf{R}) = \mathbf{O} \in \text{SO}(3)$,

$$D^{(j_k)\dagger} J_{\alpha_k} D^{(j_k)} = \sum_{\beta_k=1}^3 \mathbf{O}_{\beta_k \alpha_k} J_{\beta_k}, \quad (83)$$

we can write

$$\tilde{h}_{\alpha} = \frac{1}{\Gamma} \sum_{\beta} h_{\beta} \prod_{k=1}^N \left(\sum_{\lambda} \mathbf{O}_{\lambda_k \beta_k} \text{Tr} [J_{\lambda_k} J_{\alpha_k}] \right). \quad (84)$$

Using the relation

$$\text{Tr} [J_{\lambda_k} J_{\alpha_k}] = \frac{j_k(j_k+1)(2j_k+1)}{3} \delta_{\lambda_k \alpha_k}, \quad (85)$$

we find

$$\tilde{h}_{\alpha} = \sum_{\beta} h_{\beta} \left(\prod_{k=1}^N \mathbf{O}_{\alpha_k \beta_k} \right). \quad (86)$$

A tensor that transforms under rotations according to the previous equation is called a Cartesian tensor of rank N and dimension three [63]. Thus, the rotation-invariant component of an interaction Hamiltonian is equivalent to the component of its Cartesian tensor that is invariant under rotations, *i.e.*, under any change of coordinates. Rotationally invariant tensors are called *isotropic tensors* and are formed by a sum of products of Kronecker deltas and Levi-Civita symbols [63–65]. For ranks up to 8, Ref. [66] lists a complete set of linearly independent isotropic tensors. For two-, three- and four-body interactions, we list in Table 7 these independent isotropic tensors, the most

Rank	Linearly independent isotropic tensors	Most general isotropic Hamiltonian	Anisotropy condition
2	δ_{ij}	$\lambda \mathbf{J}^1 \cdot \mathbf{J}^2$	$\text{Tr}[h] = 0$
3	ϵ_{ijk}	$\lambda \mathbf{J}^1 \cdot (\mathbf{J}^2 \times \mathbf{J}^3)$	$\sum_{ijk} \epsilon_{ijk} h_{ijk} = 0$
4	$\delta_{ij}\delta_{kt}$ $\delta_{it}\delta_{jk}$ $\delta_{ik}\delta_{jt}$	$\lambda (\mathbf{J}^1 \cdot \mathbf{J}^2)(\mathbf{J}^3 \cdot \mathbf{J}^4)$ $+ \eta (\mathbf{J}^1 \cdot \mathbf{J}^4)(\mathbf{J}^3 \cdot \mathbf{J}^2)$ $+ \gamma (\mathbf{J}^1 \cdot \mathbf{J}^3)(\mathbf{J}^2 \cdot \mathbf{J}^4)$	$\sum_{ij} h_{iijj} = 0,$ $\sum_{ij} h_{ijij} = 0,$ and $\sum_{ij} h_{ijji} = 0$

Table 7: List of linearly independent isotropic tensors (in Cartesian coordinates) of dimension three and rank 2, 3 and 4, and the corresponding most general multilinear isotropic Hamiltonian and anisotropy conditions on the interaction tensor (81).

general isotropic Hamiltonian and necessary and sufficient conditions for a given interaction tensor to have no isotropic component, which we call *anisotropy conditions*.

In the case where we are interested in a $K < N$ interaction between N spins, the isotropic tensors, and therefore the anisotropy conditions, are equivalent to those obtained in K interactions between K spins. The only difference is that the isotropic tensors must be multiplied by $N - K$ identity operators. The anisotropy conditions for the K -body terms of K spins define $\binom{N}{K}$ anisotropy conditions for the K -body terms of N spins, each of which is associated with the choice of K spins interacting among the N spins.

E.2 Arbitrary two-body interactions

Consider now a two-body interaction Hamiltonian between two spins of quantum numbers $j_1 \leq j_2$. The most general Hamiltonian belongs to (see Sec. 6)

$$H \in \bigoplus_{\mathbf{L}} \mathcal{B}_{j_1}^{(L_1)} \otimes \mathcal{B}_{j_2}^{(L_2)} = \bigoplus_{\mathbf{L}} \bigoplus_{\tilde{\mathbf{L}}_{\mathbf{L}}} \tilde{\mathcal{B}}^{\tilde{\mathbf{L}}_{\mathbf{L}}}, \quad (87)$$

with $\mathbf{L} = (L_1, L_2)$ and where L_k runs from 0 to $2j_k$ and $\tilde{\mathbf{L}}_{\mathbf{L}}$ from $|L_1 - L_2|$ to $L_1 + L_2$. As we explained in Sec. 6, the anisotropy conditions are related to the 0-irrep subspaces which only appear for $L_1 = L_2$. There are therefore $2j_1 + 1$ different rotation-invariant subspaces in $\mathcal{B}_{j_1}^{(L)} \otimes \mathcal{B}_{j_2}^{(L)}$ for $L = 0, \dots, 2j_1$. Their exact expressions can be calculated using the theory of addition of angular momentum [33]; the spin-0 state formed from two spin- L states is given by

$$\begin{aligned} & \sum_{M_1, M_2 = -L}^L C_{LM_1 LM_2}^{00} |L, M_1\rangle \otimes |L, M_2\rangle \\ &= \frac{(-1)^L}{\sqrt{2L+1}} \sum_{M=-L}^L (-1)^{-M} |L, M\rangle \otimes |L, -M\rangle, \quad (88) \end{aligned}$$

where $C_{LM_1 LM_2}^{00} = (-1)^{L-M_1} \delta_{M_1, -M_2} / \sqrt{2L+1}$ is a Clebsch-Gordan coefficient. We now replace the states $|L, M\rangle$ by the multipolar tensors T_{LM} . The

resulting operators, denoted as

$$I_L \equiv \sum_{M=-L}^L \frac{(-1)^{-M}}{\sqrt{2L+1}} T_{LM} \otimes T_{L-M}, \quad (89)$$

are $\text{SU}(2)$ invariant because they will transform as the corresponding spin-0 state. All I_L are linearly independent and I_0 is proportional to the identity. Thus, a Hamiltonian free of rotationally invariant components except the identity must fulfill $2j_1$ anisotropy conditions given by

$$\text{Tr}(I_L H) = 0, \quad L = 1, \dots, 2j_1. \quad (90)$$

For the case of a multispin system with more than two parties, H must satisfy the same conditions for any pair of constituents.

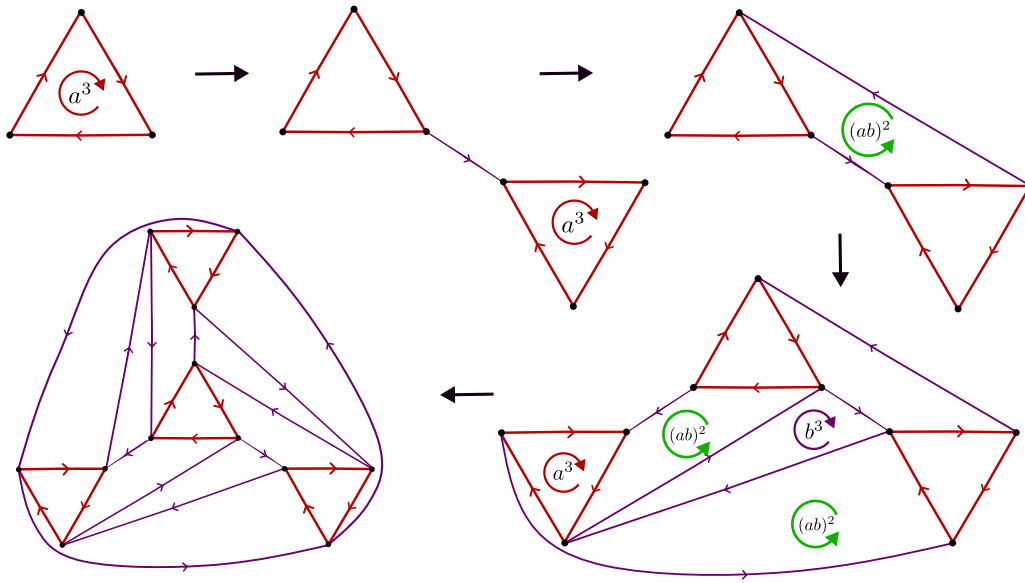


Figure 7: Construction process of the Cayley graph of $\mathcal{G} = \langle a, b \mid a^3, b^3, (ab)^2 \rangle$. Each loop corresponds to a defining relation and is added one by one until every vertex has the right number of outgoing and incoming edges. Edges of color red (resp. purple) refer to the generator a (resp. b).

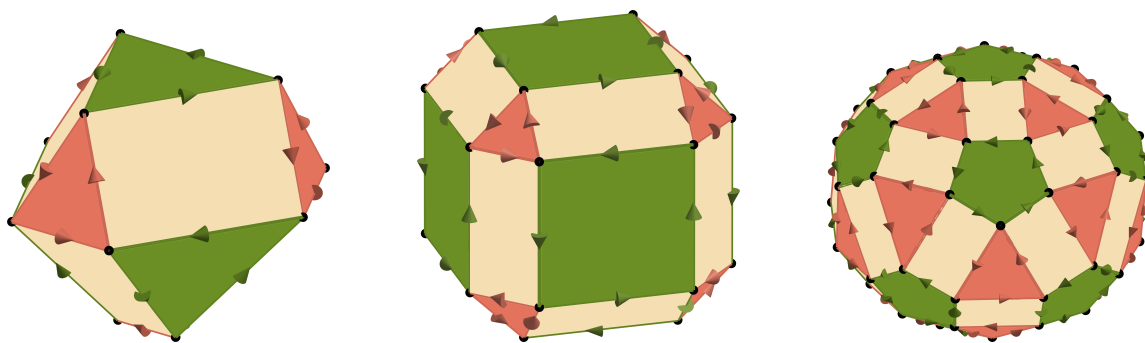


Figure 8: Three-dimensional representation of the Cayley graph of the groups (left) $T = \langle a, b \mid a^3, b^3, (ab)^2 \rangle$, (middle) $O = \langle a, b \mid a^4, b^3, (ab)^2 \rangle$ and (right) $I = \langle a, b \mid a^5, b^3, (ab)^2 \rangle$. The generator a (resp. b) is represented by a green (resp. red) arrow. Each colored surface corresponds to a loop generated by one of the defining relations.